Probing matter under extreme conditions at Fermi@Elettra: the TIMEX beamline

Andrea Di Cicco*

TIMEX collaboration

C. Masciovecchio, E. Principi, F. D'Amico et al.
(Sincrotrone Trieste)
R. Gunnella **(Università di Camerino)*
A. Filipponi *(Università dell'Aquila)*

Forthcoming radiation sources

- Many new sources operating or under construction based on the free-electron-laser (FEL) concept (FLASH, LCLS, XFEL, FERMI, SCSS...), delivering VUV/soft and hard x-ray ultrashort pulses of extremely intense and collimated (coherent) radiation.
- FLASH has been the first operating free-electron laser for VUV and soft X-ray radiation (2005 to now). Wavelength range 6.5 nm to about 50 nm with GW peak power and pulse durations between 10 fs and 50 fs.
- FEL radiation is obtained either using the SASE process (self-amplified spontaneous emission) which produces an intrinsic noise in the pulse (lack of time coherence) or through an optical laser seeding (time coherence is forced by the laser seed).
- The current challenge is a suitable exploitation of the potential of these new sources which poses new problems in physics and technology. Due to the high energy density contained in each photon pulse these new sources are naturally suitable to explore highly excited states (matter under extreme conditions).

FERMI: a seeded Free Electron Lasers Source for Users Experiments

Courtesy of Enrico Allaria – Dec 2010

FERMI at the Elettra Laboratory

Civil engineering
"Main FERMI" construction began
25 March 2009

Completed by June 2010

FEL1 LINAC installed in Aug. 2010

FEL1 undulators installed in Oct-Nov. '10

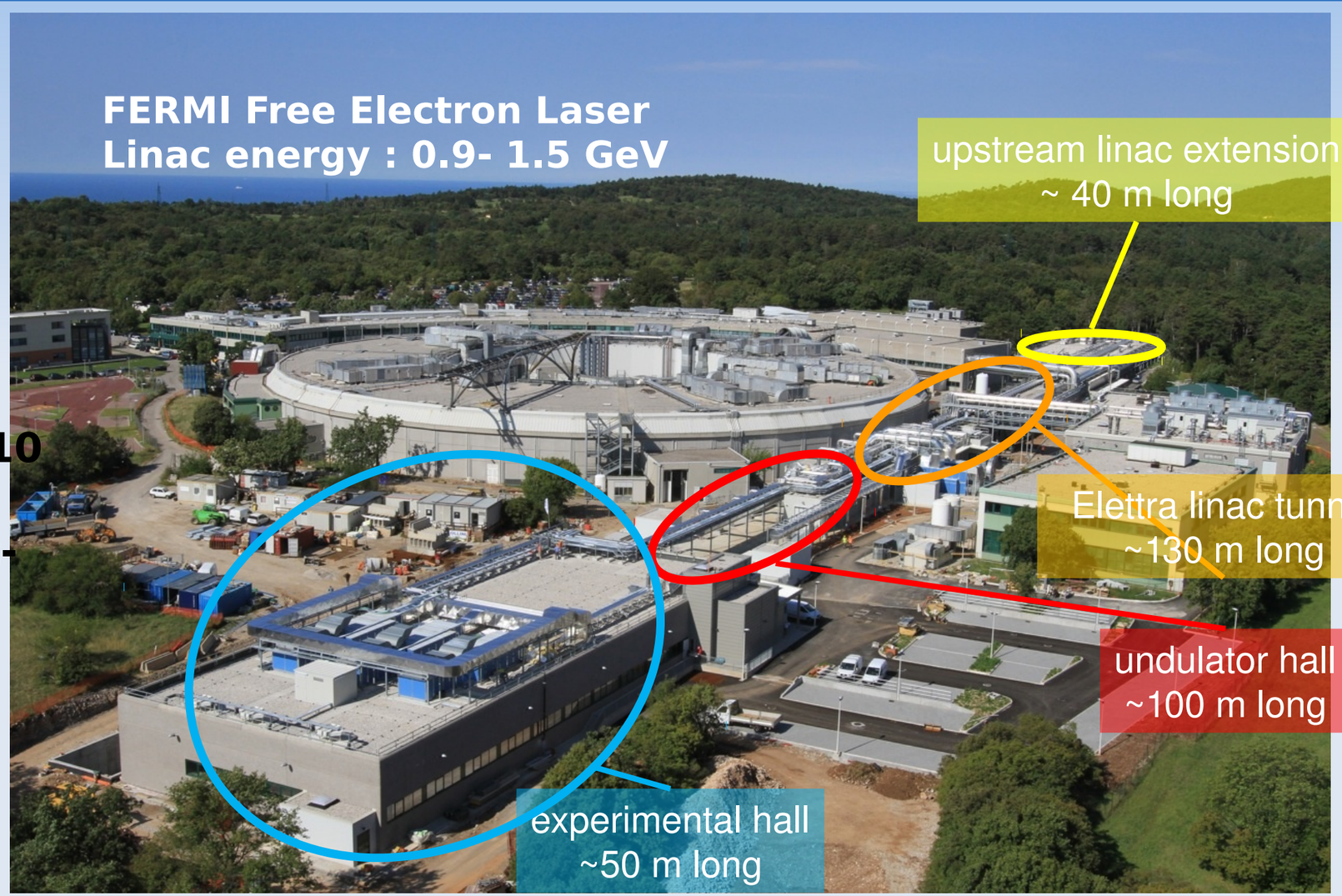

Fermi main features

- **FERMI@Elettra single-pass seeded FEL user-facility. Two separate FEL amplifiers (FEL1 and FEL2) will cover the spectral range from 100 nm (12eV) to 4 nm (320 eV), first harmonic.**
- **Based on the high gain harmonic generation scheme the two FEL will provide users with photon pulses of about 100fs with unique features.**

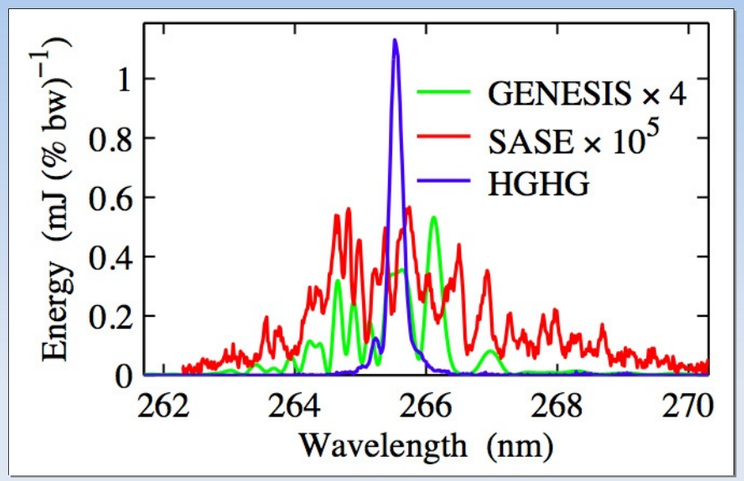

❑	high peak power	0.3 – GW's range
❑	short temporal structure	sub-ps to 10 fs time scale
❑	tunable wavelength	var. gap APPLE II-type undulators
❑	variable polarization	horizontal/circular/vertical
❑	seeded harm. Cascade	strong long. and transv. coher.

Li-Hua Yu
DUV-FEL,
Brookhaven

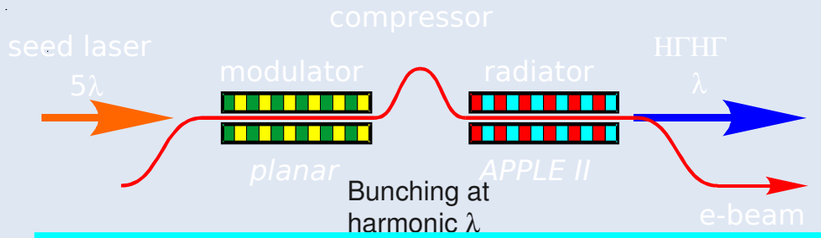

High Gain Harmonic Generation - HGHG

FEL1 and FEL2

FEL-1(operating), based on a single stage high gain harmonic generations scheme initialized by a UV laser will cover the spectral range from ~100 nm down to 20nm. FEL1 operated since Dec 2010 in the 65-24 nm range increasing gradually the peak brightness to the expected performances..

FEL-2 (under construction): in order to be able to reach the wavelength range from 20 to ~4 nm starting from a seed laser in the UV, will be based on a double cascade of high gain harmonic generation. The nominal layout will use a magnetic electron delay line in order to improve the FEL performance by using the fresh bunch technique.

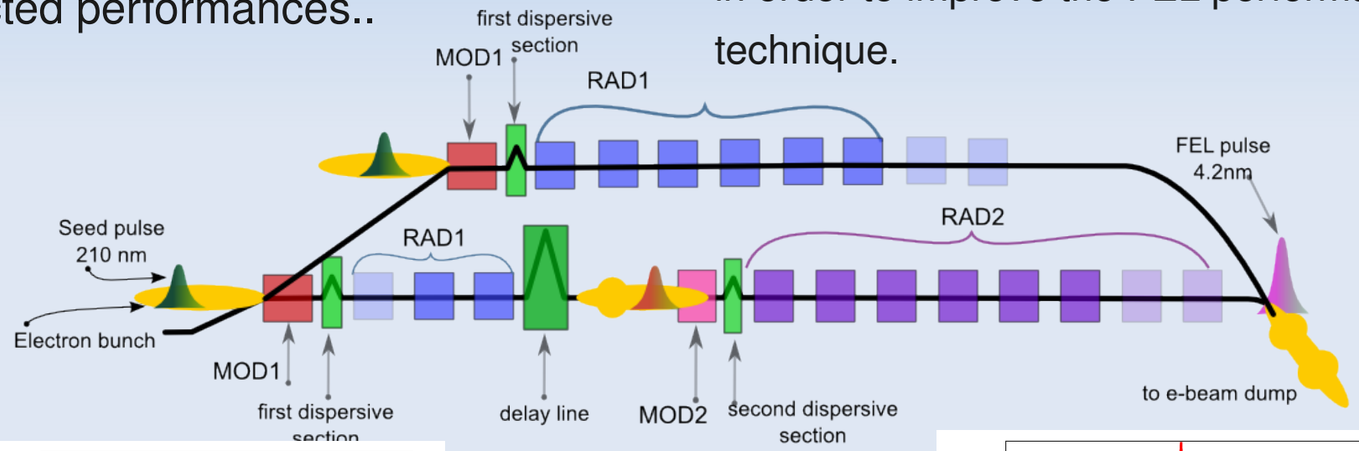

FEL1

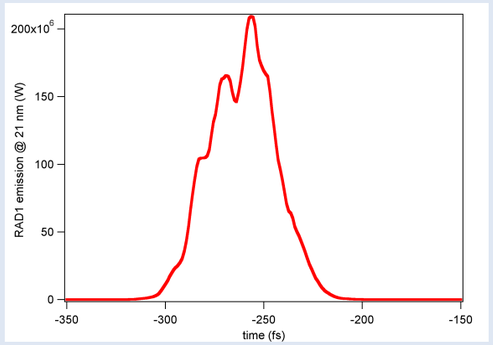

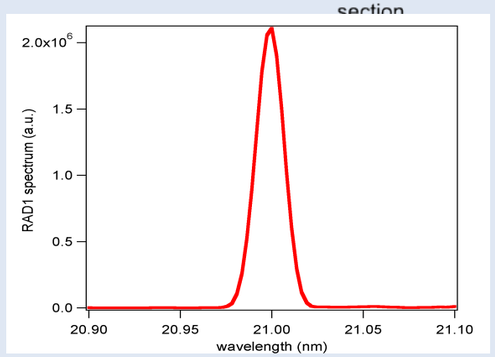

FEL2

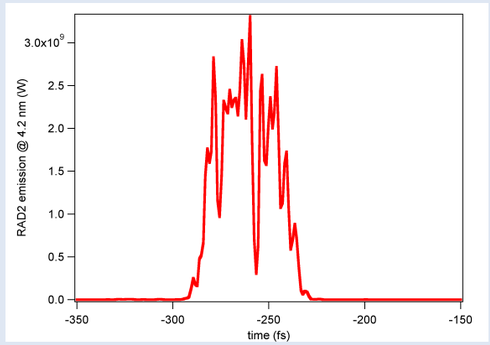

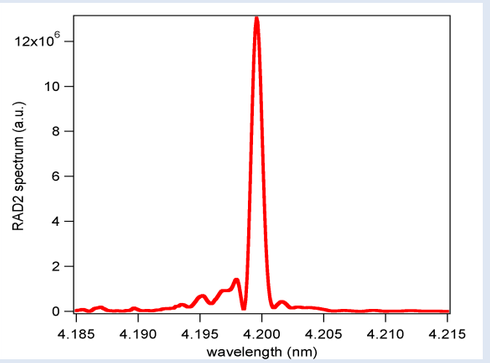

Fermi FEL output parameters

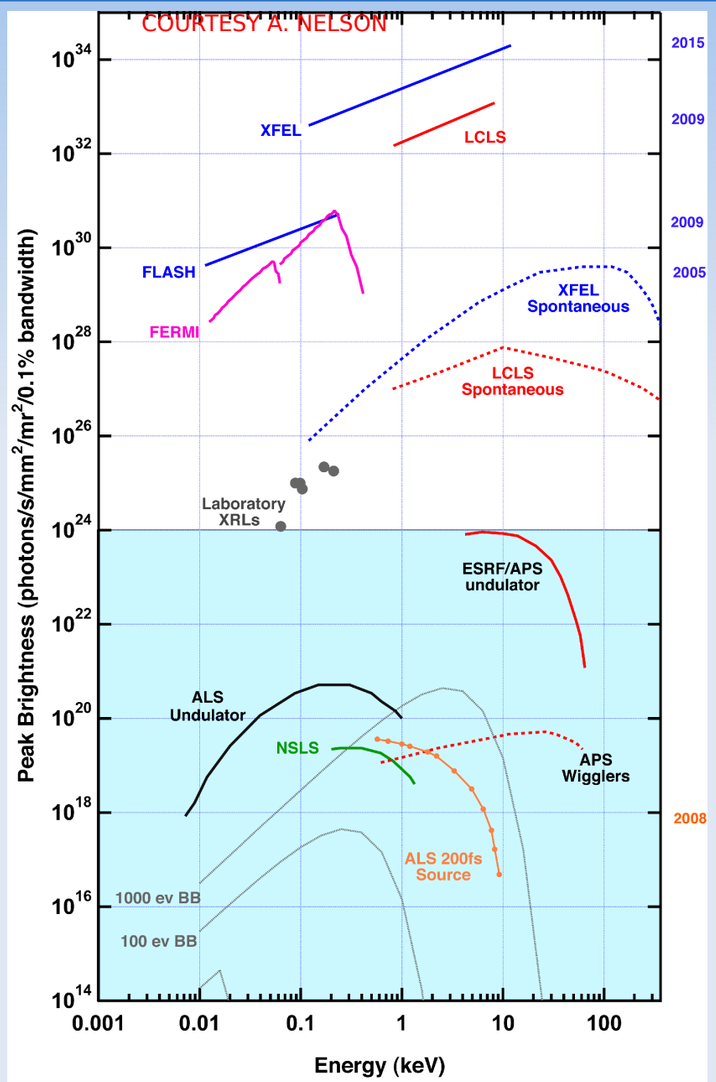

- Peak brightness of FELs are several order of magnitude higher of those of synchrotrons.
- Slow repetition rates for current FELs (10-200 Hz as compared to ~100 MHz in storage rings) limits the average flux.
- Single-shot experiments using time structure, intensity (coherence, polarization).

λ (nm)	FEL	Harmonic	Flux @ source (ph/pulse)	Flux @ sample (ph/pulse)	Fluence (W/cm^2)
1	2	3rd	1.5×10^{8}	1.9×10^{6}	2.6×10^{11}
1.4	2	3rd	9.3×10^{9}	2.0×10^{8}	1.1×10^{13}
1.67	2	3rd	9.3×10^{9}	2.4×10^{8}	1.0×10^{13}
3	2	1st	3.5×10^{11}	4.7×10^{10}	2.1×10^{15}
3.3	2	3rd	5×10^{10}	1.9×10^{9}	7.8×10^{13}
4	1	3rd	1×10^{9}	4.3×10^{7}	3.4×10^{11}
4.2	2	1st	1.8×10^{12}	3.4×10^{11}	5.6×10^{15}
5	2	1st	3.3×10^{12}	8×10^{11}	1.1×10^{16}
6.7	1	3rd	1×10^{11}	1.6×10^{10}	7.6×10^{13}
10	2	1st	1×10^{13}	6.6×10^{12}	9.0×10^{16}
20	2	1st	5×10^{13}	3.3×10^{13}	2.3×10^{17}
20	1	1st	1×10^{13}	4.9×10^{12}	7.9×10^{15}
40	1	1st	4×10^{13}	2.0×10^{13}	1.6×10^{16}
80	1	1st	2×10^{14}	9.8×10^{13}	3.9×10^{16}

Courtesy of F. Parmigiani, W. Fawley & E. Allaria

Fermi@Elettra FEL source

- *Fermi@Elettra is a free-electron source in Trieste. The FEL1 is presently in the final commissioning stage (expected routine operation starting in May 2012).*

The FEL1/FEL2 photon beams are delivered to the beamlines through the PADReS (Photon Analysis Delivery and Reduction System). This will includes gas monitor detectors and attenuators, mirror switching, x-ray spectrometers.

Parameter	FEL - 1	FEL - 2	Units
Wavelength	100 - 20	20 - 3	nm
Photon Energy	12 - 62	62 - 413	eV
Pulse Length	30 - 100	< 100	fs
Bandwidth	~ 20 - 40	~ 20 - 40	meV
Polarization	variable	variable	-
Repetition Rate	10 - 50	10 - 50	Hz
Peak Power	1 ÷ 5	~ 1	GW
Photons per Pulse	$2 \cdot 10^{14}$ @ 100 nm	$1 \cdot 10^{13}$ @ 10 nm	-
Power Fluctuation	~ 25%	> 50%	-
Central Wavelength Fluctuation	within bandwidth	within bandwidth	-
Output Transverse Position Fluctuation	50	50	µm
Pointing Fluctuation	< 5	< 5	µrad
Output Spot Size (intensity, FWHM@waist)	290	140	µm
Divergence (intensity, RMS)	50 @ 40 nm	15 @ 10 nm	µrad

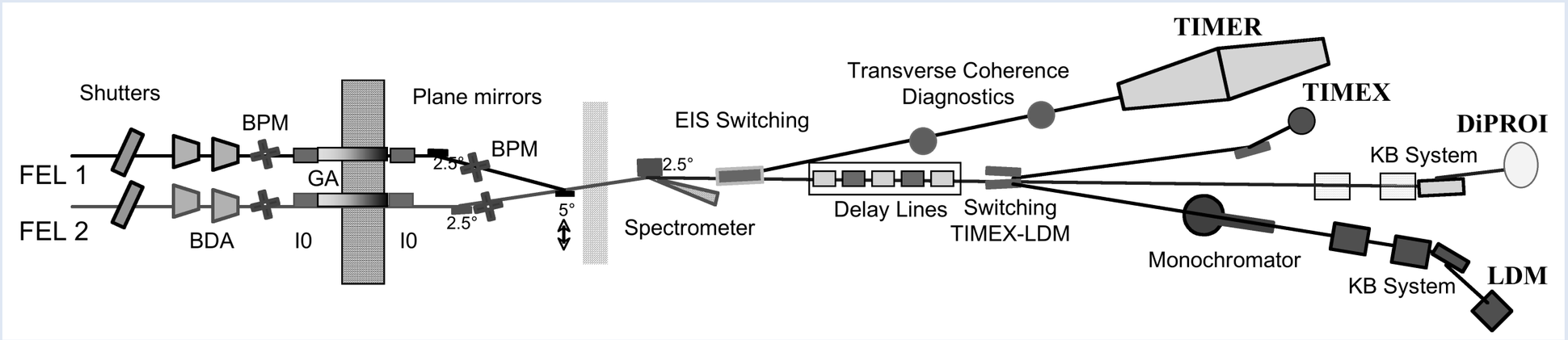

Photon delivery to beamlines

The photon beam delivered alternatively by the two FEL sections (FEL1 and FEL2) is collected, analyzed, and re-directed to the following beamlines in the Experimental Hall by the PADReS section.
The **PADReS** (Photon Analysis Delivery and Reduction System) is located between the undulators and the main Switching Chambers. For each FEL it includes (going downstream):

- Front-End section (x-ray slits, shutter, and radiation stopper)
- Gas Monitor Detector 1 (GMD1): I_0 monitor and Beam Position Monitor
- Gas Attenuator (GA)
- Gas Monitor Detector 2 (GMD2): I_0 monitor and Beam Position Monitor
- Radiation Absorbtion Mirrors (RAM)
- X-ray spectrometer

A common Switching Chamber (SC) directing to the beamlines the beams coming from both FELs is located at the end of the section.

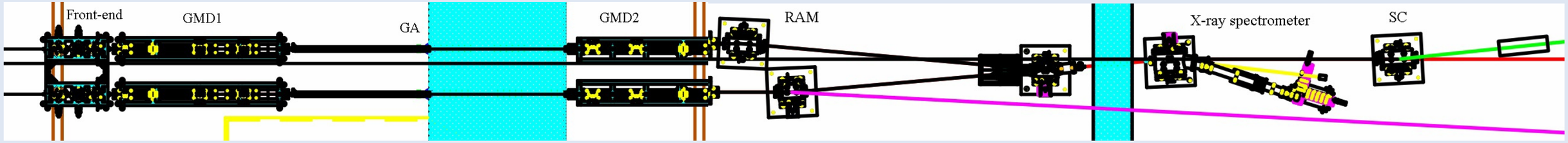

PADReS layout: Front-end, GMDs, GA, RAM, x-ray spectrometers, SC

Note: not ALL the devices are currently installed (end 2011).

Beamlines

Three beamlines are designed in order to serve three separate endstations dedicated to different scientific areas: **Low Density Matter** (LDM), **Elastic and Inelastic Scattering** (EIS), and **DIffraction and PRojection Imaging** (DIPROI). The beamlines start after the PADReS. The movable LDM monochromator can be inserted to direct the beam to the LDM endstation. If retracted, it allows the beam travel to the EIS Switching Mirror where it is possible to select between the EIS and the DiProI endstations. A further insertable mirror can direct the beam either to the EIS or the TIMEX experiments.

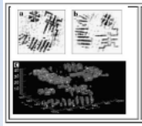

DIPROI - DIffraction and PRojection Imaging

The microscopy beamline will host an experimental station for coherent DIfraction and PROjection Imaging, DIPROI, adapted for research in various domains in a single shot

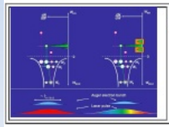

LDM - Low Density Matter

The advent of free electron lasers enables the exploration of a new ultrafast-ultrasmall frontier in atomic and molecular physics. It is possible to control outer-shell electron dynamics with intense ultrafast optical lasers along with inner-shell processes by combining intense infrared/optical lasers with tunable sources of XUV and x-ray radiation.

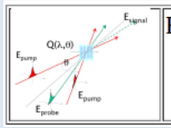

EIS - Elastic and Inelastic Scattering

TIMEX and TIMER

1) TIME-Resolved spectroscopy of mesoscopic dynamics in condensed matter (TIMER);
2) Ultrafast TIme-Resolved Studies of Matter under EXtreme and Metastable Conditions (TIMEX).

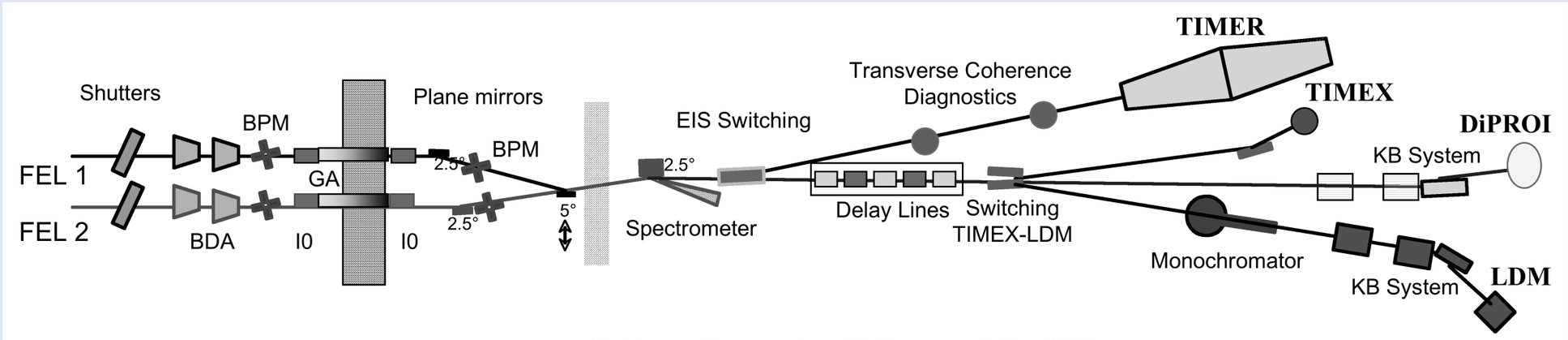

Motivations and aims of the TIMEX end-station

(TIMe-resolved studies of Matter under EXtreme and metastable conditions)

•The Fermi@Elettra clean 0.1-1 ps pulses in the 10-400 eV range (or higher using harmonics) are able to raise solid matter at temperatures up to 10 eV in very short times compared to hydrodynamic expansion. This opens the way to investigate fundamental properties of *warm dense states in bulk-like thin films and layers*. Moreover, it can be used to probe *metastable and non equilibrium thermodynamic* conditions with an unprecedented temporal resolution.

•The FEL beam will be used either as a pump or as a probe for time-resolved studies of the optical and soft x-ray properties of matter accessing microscopic electronic and dynamical structure information on excited states. Typical experiments share similar needs, including time-resolved reflectivity, transmission, deposited energy measures.

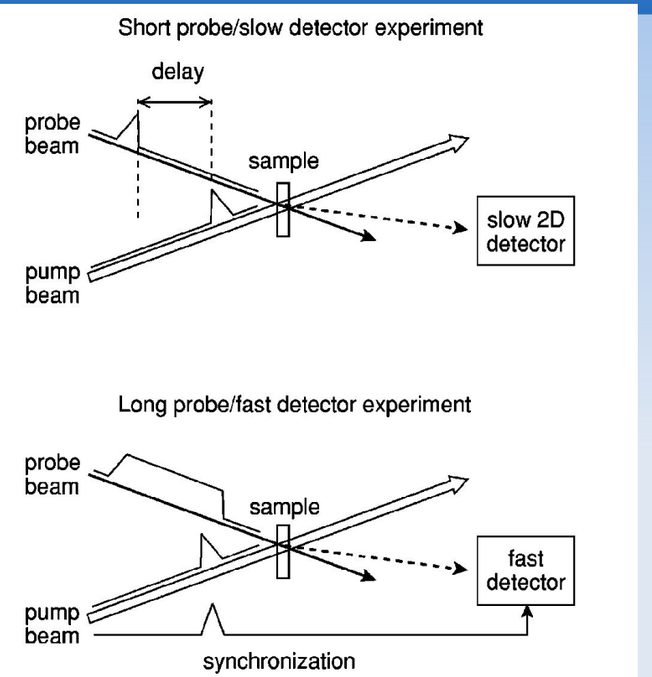

FIG. 3. Two types of pump-probe experiments.

- *TIMEX is intented to be a versatile instrument, suitable for time-resolved experiments under controlled conditions. It is conceived to allow ultrafast studies (transmission, reflectivity/absorption) of*
- *(i) warm dense matter.*
- *(ii) transitions occurring in stable, metastable and excited states under extreme conditions.*
- *(iii) extension to study of ablation phenomena, surface melting*

`

FEL radiation is able to create and/or probe Warm Dense Matter (WDM) in an extended P-T range

- **WDM is a region in the temperature -density diagram: present in core of large planets and in experiments relevant to inertial fusion, in the transition from solids to plasma**

•*4th generation light sources with large numbers of photon/bunch and sub-picosecond pulses:*
FEL source as a pump for generation of bulk WDM (but also probe under certain conditions)
•*perform single-shot experiments with reasonable statistics*

•*Present experimental data, largely based on shock-wave techniques probing matter along the Hugoniot, show that theories are not able to reproduce EOS.*

•*During WDM creation, systems usually start solid and end as a plasma. FEL radiation can heat matter rapidly and uniformly to create isochores (costant density- red) and isoentropies on release (constant entropy -blue).*

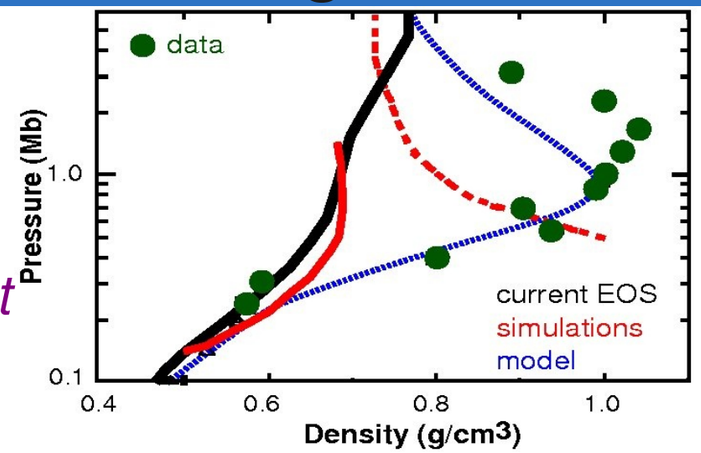

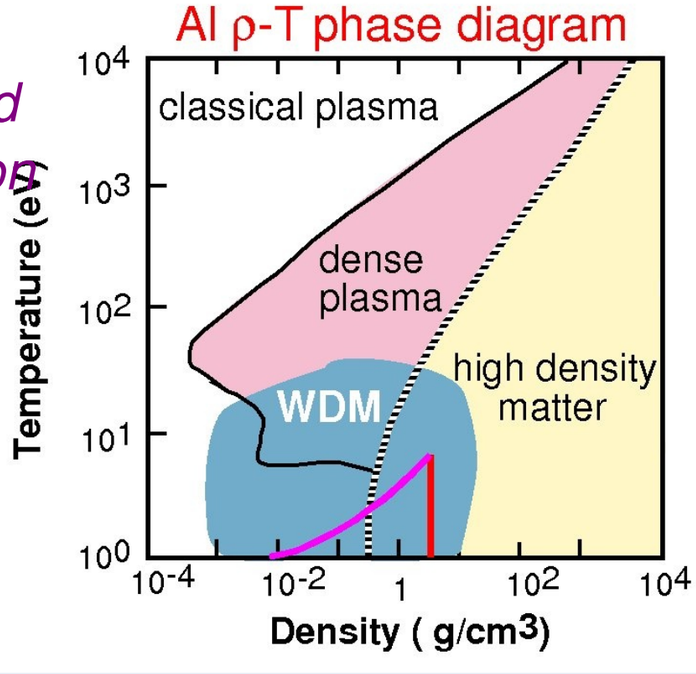

High temperature/pressure studies of condensed matter under transient conditions

- A variety of experiments are possible exploiting isochore ultrafast heating reaching extreme conditions.
- Example of Carbon: fluid condensed phases exists only at high pressures (sublimation below 100 bars, typical T> 4000 K). Experiment presently impossible under static conditions. Previous optical fs spectroscopy measurements indicate fluid C as a poor metal (Nature 356, 110, 1992; PRB 45, 2677, 1992). Recent ultrafast XAS data indicate a sp-bonded structure of the low density liquid (PRL 94, 05740, 2005). A transition line between low-density and high density liquids could be identified.

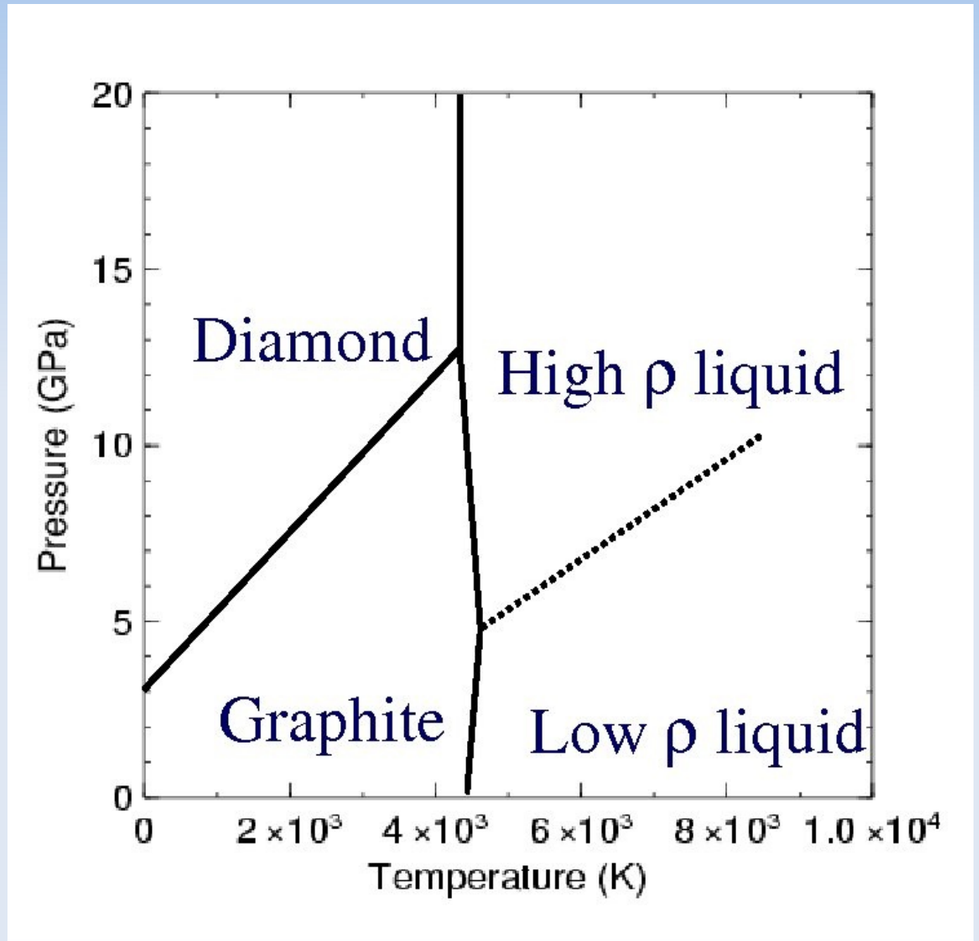

Measuring properties in a No Man's Land

- *Example of experiments on condensed matter under highly metastable or non-equilibrium conditions.*
- *High density-low density (metal-semiconducting) polymorphism in C/Si/Ge/H_2O and related compounds. Often hidden in an unaccessible region!*
- *Ultrafast heating of a bulk amorphous sample using the FEL beam can be used to probe highly undercooled, presently unreachable, states.*
- *Access to various properties including dynamics of melting and crystallization.*
- *Various techniques possible in combination with pulsed lasers: reflectivity, transmission, scattering.*

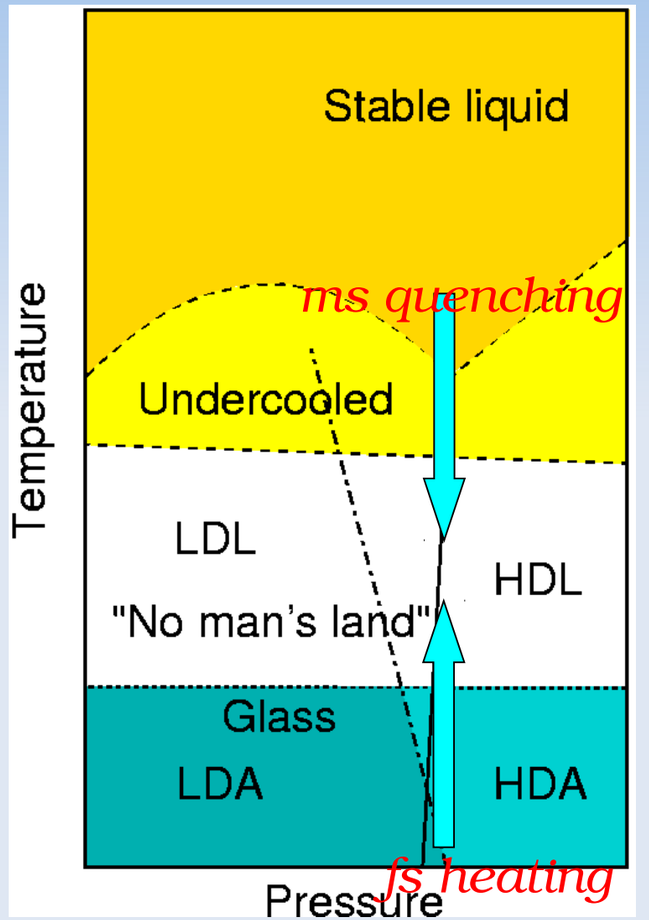

Surface melting phenomena

- Undercooled liquids are easily obtained, overheated solids are extremely difficult. The general phenomenon is explained by the existence of a wet surface well below the melting point, providing the initial germ for melting.
- Scattered experimental studies deal with microscopic details of the surface melting processes under high temperature conditions, nothing about the dynamics of this transition.
- *FEL radiation can be used to induce and study ultrafast melting of surfaces*
- Pilot static experiment results: Surface melting is limited to 3 atomic layers in Si(001) while it proceeds much faster (5 layers at 1500 K) in Si(111)
- The different vibrational amplitudes of the outermost atoms at the Si(111) may be responsible of this different behaviour. Metalization is extended to deeper layers as compared to the solid-liquid interface

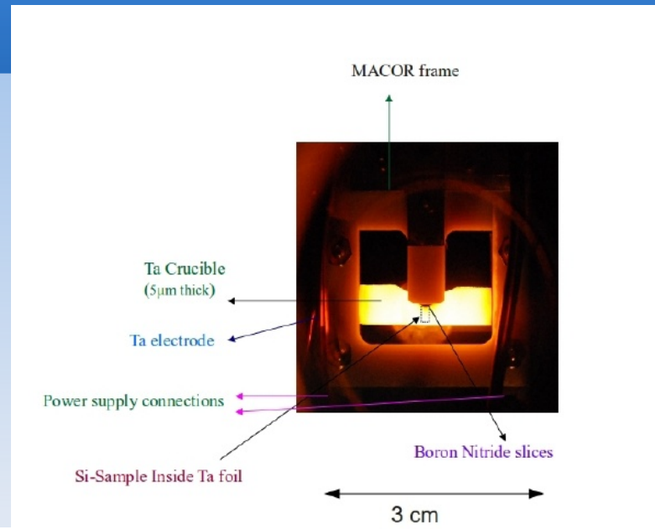

PHYSICAL REVIEW LETTERS

Depth Profiling of Melting and Metallization in Si(111) and Si(001) Surfaces

R. Gunnella,[1] M. Ali,[1,*] M. Abbas,[1,†] F. D'Amico,[2,1] E. Principi,[2,1] and A. Di Cicco[1,‡]
[1]*CNISM, Sez. Fisica, Scuola di Scienze e Tecnologie, Università di Camerino, via Madonna delle Carceri, I-62032 Camerino (MC), Italy*
[2]*Synchrotron ELETTRA, Strada Statale 14 - I-34149 Basovizza, Trieste, Italy*
(Received 9 February 2011)

An original approach for measuring the depth profile of melting and metallization of the Si(111) and Si(001) surfaces is proposed and applied. The different probing depths of the Auger electron and electron energy loss (EELS) spectroscopies are exploited to study the number of molten and metallic layers within 5–30 Å from the surface up to about 1650 K. Melting is limited to 3 atomic layers in Si(001) in the range 1400–1650 K while the number of molten layers grows much faster (5 layers at about 1500 K) in Si(111) as also indicated by the L_3-edge shift observed by EELS. The relationship between melting and metallization is briefly discussed.

TIMEX beamline layout

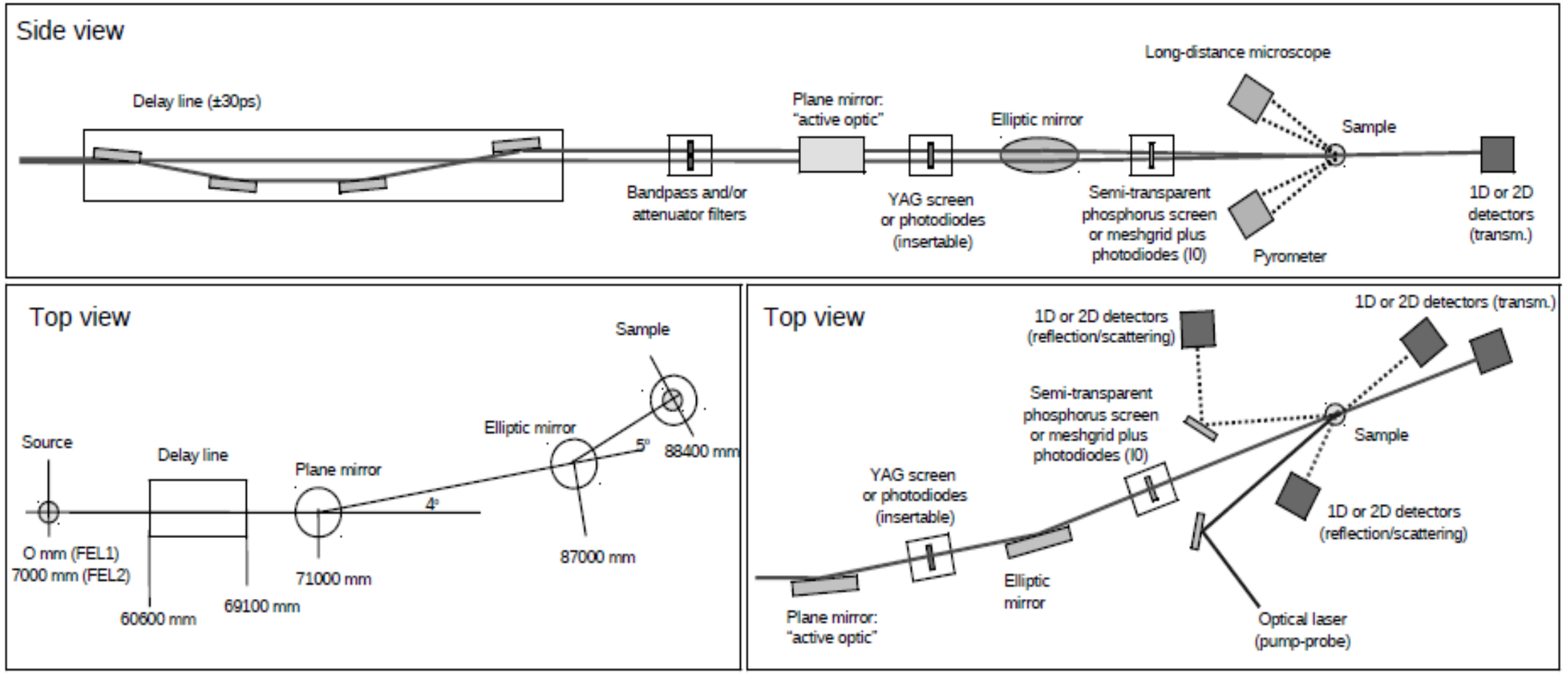

Figure 1. Sketch of the TIMEX end-station under commissioning at the FERMI@Elettra FEL facility. The side view shows all the optical elements up to the sample chamber, most of them presently under construction. In the top view on the left side of the figure we show the main components of the end-station along with their distances from the sources. In the top view, right side, we show the details of the focusing and aligning devices and the detectors used for reflection and transmission measurements using both the FEL and a probe pulse of an optical laser.

TIMEX layout details

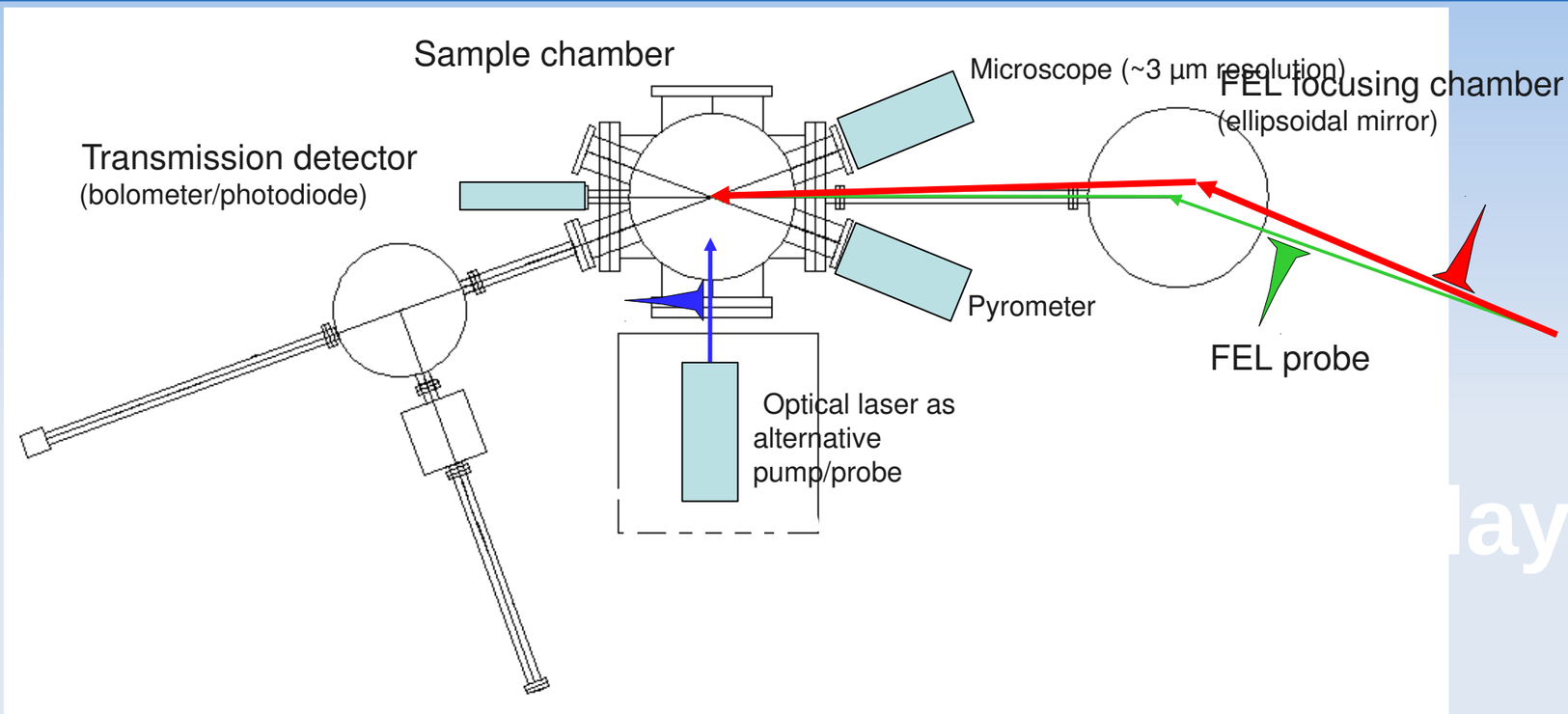

- *The flexible set-up of the Timex end-station can host different experimental configurations.*

- *Details on the experimental layout and pilot pump and probe experiments are reported in the papers of the Timex collaboration*

Damage to VUV, EUV, and X-ray Optics III, edited by Libor Juha, Saša Bajt, Richard A. London,
Proc. of SPIE Vol. 8077, 807704 · © 2011 SPIE · CCC code: 0277-786X/11/$18 · doi: 10.1117/12.887633

Invited Paper

Probing matter under extreme conditions at FERMI@Elettra: the TIMEX beamline

Andrea Di Cicco[a], Filippo Bencivenga[b], Andrea Battistoni[b], Daniele Cocco[b], Riccardo Cucini[b], Francesco D'Amico[b], Silvia Di Fonzo[b], Adriano Filipponi[c], Alessandro Gessini[b], Erika Giangrisostomi[b], Roberto Gunnella[a], Claudio Masciovecchio[b], Emiliano Principi[b], and Cristian Svetina[b]

Journal of Non-Crystalline Solids 357 (2011) 2641–2647

Probing phase transitions under extreme conditions by ultrafast techniques: Advances at the Fermi@Elettra free-electron-laser facility

Andrea Di Cicco [a,b,c,*], Francesco D'Amico [b], Goran Zgrablic [b], Emiliano Principi [a], Roberto Gunnella [a], Filippo Bencivenga [b], Cristian Svetina [b], Claudio Masciovecchio [b], Fulvio Parmigiani [b], Adriano Filipponi [d]

Focusing the pulse

·**FOCUSING capabilities down to a few µm spot**

Focusing ellipsoidal mirror with focal length of about 1.4 m (source distance optimized for FEL2)

·**Beam-shaping**

"active" beam-shaping 400 mm (multi-piezo-patches for bending) mirror for obtaining Lorentzian-like profiles

Nuclear Instruments and Methods in Physics Research A 635 (2011) S12–S15

A beam-shaping system for TIMEX beamline

C. Svetina [a,*], G. Sostero [a], R. Sergo [a], R. Borghes [a], C. Callegari [a], F. D'Amico [a], F. Bencivenga [a], C. Masciovecchio [a], A. Di Cicco [b,c], D. Cocco [a]

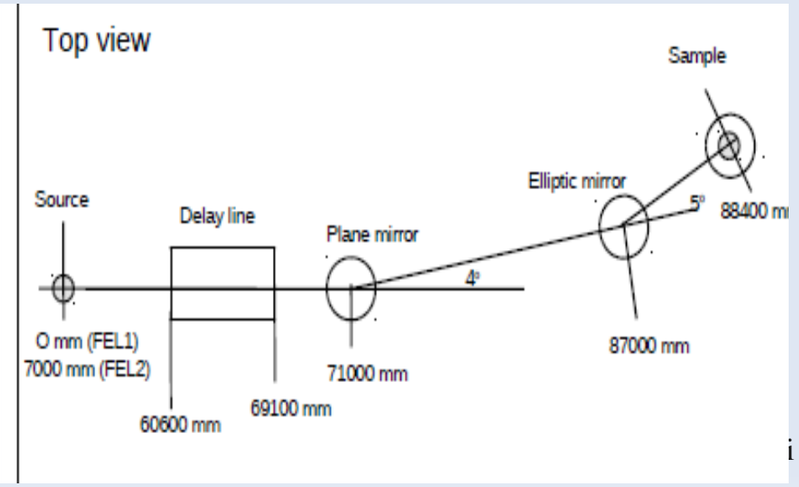

Table 2
Requirements for the TIMEX focusing ellipsoidal mirror.

Parameter	Value
Source distance p (m)	61.5
Focal length q (m)	1.4
Incidence angle α (°)	2.5
Tangential slope error rms (µrad)	< 1
Sagittal slope error rms (µrad)	< 5
Coating	Ir (50 nm)
Surface roughness (nm)	< 0.3

Table 3
Beam parameters at the sample position for TIMEX end-station, calculated by considering the source parameters, the geometrical and reflectivity losses of all optical elements considering 1 µrad rms slope errors on the mirrors.

Wavelength (nm)	FEL	Harmonic	Spot size$_{FWHM}$ (µm × µm)	Flux (Ph/pulse)	Fluence W/cm^2
1.7	2	3rd	3.0×3.0	5.9×10^{8}	3.0×10^{13}
3.3	2	3rd	3.2×3.1	3.4×10^{9}	7.6×10^{13}
4	2	1st	3.3×3.1	1.9×10^{11}	2.9×10^{15}
6.7	1	3rd	5.1×5.1	2.2×10^{10}	8.0×10^{13}
10	2	1st	3.3×3.0	6.9×10^{12}	4.5×10^{16}
20	2	1st	4.2×3.7	2.8×10^{13}	5.8×10^{16}
20	1	1st	6.1×5.7	6.5×10^{12}	5.9×10^{15}
60	1	1st	6.7×5.7	5.4×10^{13}	1.4×10^{16}
100	1	1st	7.1×6.7	1.1×10^{14}	1.4×10^{16}

Mastering the shape of the spot

The shape of the spot can be modified by a suitable change of the plane mirror shape (obtained by 16 piezo-actuators).

We have verified that the mirror can reproduce a quasi-Lorentzian shape

$$L_\alpha(x)\,[\gamma, A, x_0] = A\frac{\gamma^{\alpha-1}}{\pi\left[(x-x_0)^\alpha + \gamma^\alpha\right]}$$

Producing spots with flat-top shapes (with or without tails) useful for the experiments

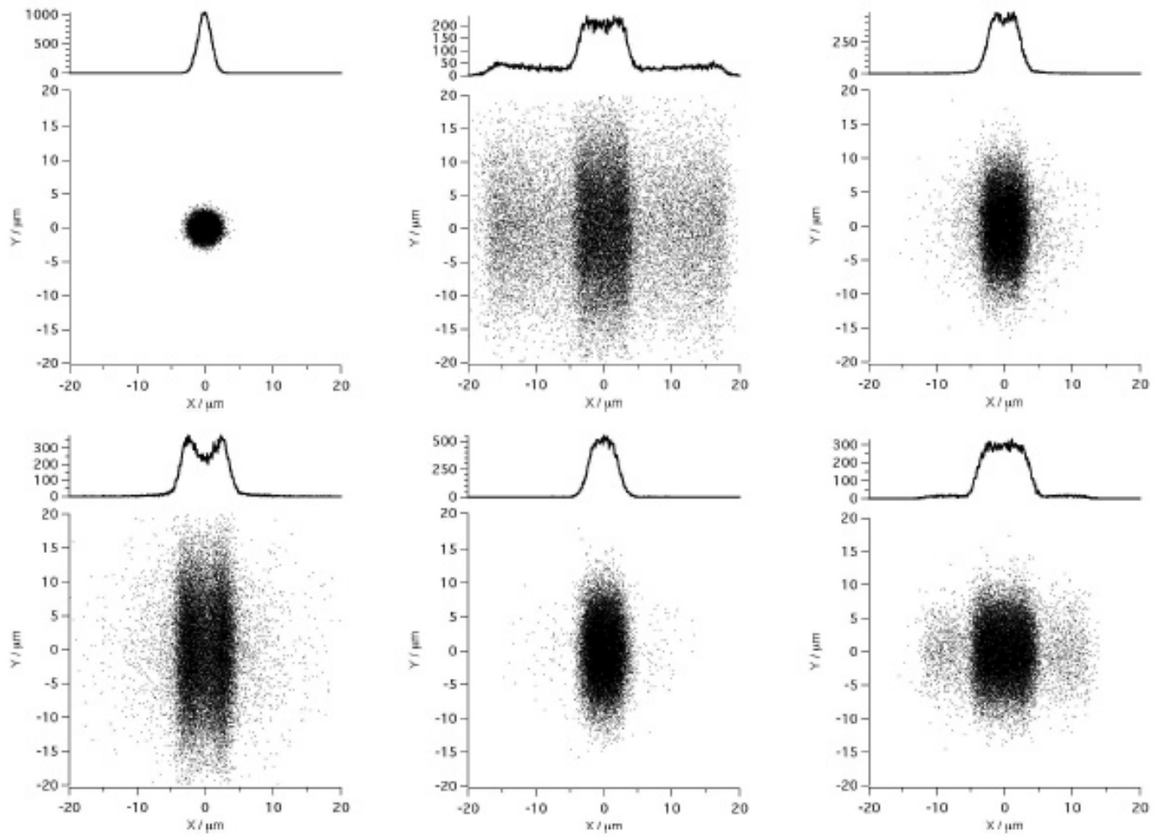

Figure 2. Ray-tracing results of the expected spots at focus with the relative mirror profiles for a wavelength of 5 nm and a divergence of 7.5 μrad. Figures on the upper row from left to right: i) ideal plane mirror (Gaussian distribution); ii) γ= 4 cm, α= 8, A= 100 nm (flat-top distribution with tails); iii) γ= 8 cm, α= 2 A= 150 nm (flat-top/double peak). Bottom, from left to right: i) γ= 8 cm, α= 2, A= 250nm (double peak); (ii) γ= 8cm, α= 4, A= 150 nm (flat-top distribution), (iii) γ= 8 cm, α= 8, A= 150 nm (larger flat-top distr.). The mirror profile is assumed to be Lorentzian-like (see text) along the x direction (x_0=0 cm).

Expected deposited energy

The deposited energy can be tuned by changing the intensity and wavelength of the FEL pulse. Strong saturation effects are obtained for high intensities (and large absorption cross sections).
Saturation can be used as a device for homogeneous bulk heating!

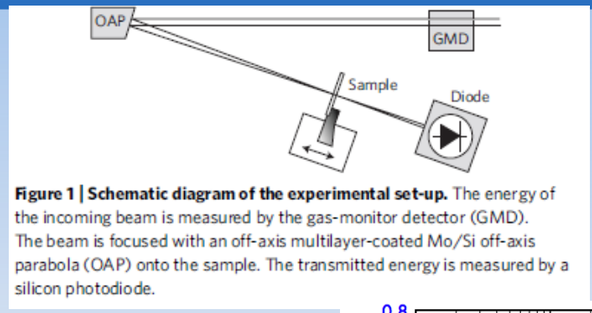

Figure 1 | Schematic diagram of the experimental set-up. The energy of the incoming beam is measured by the gas-monitor detector (GMD). The beam is focused with an off-axis multilayer-coated Mo/Si off-axis parabola (OAP) onto the sample. The transmitted energy is measured by a silicon photodiode.

52 nm Al foil (+20 nm oxide layer), 92 eV photons

Effect takes place on 15-25 fs time scale

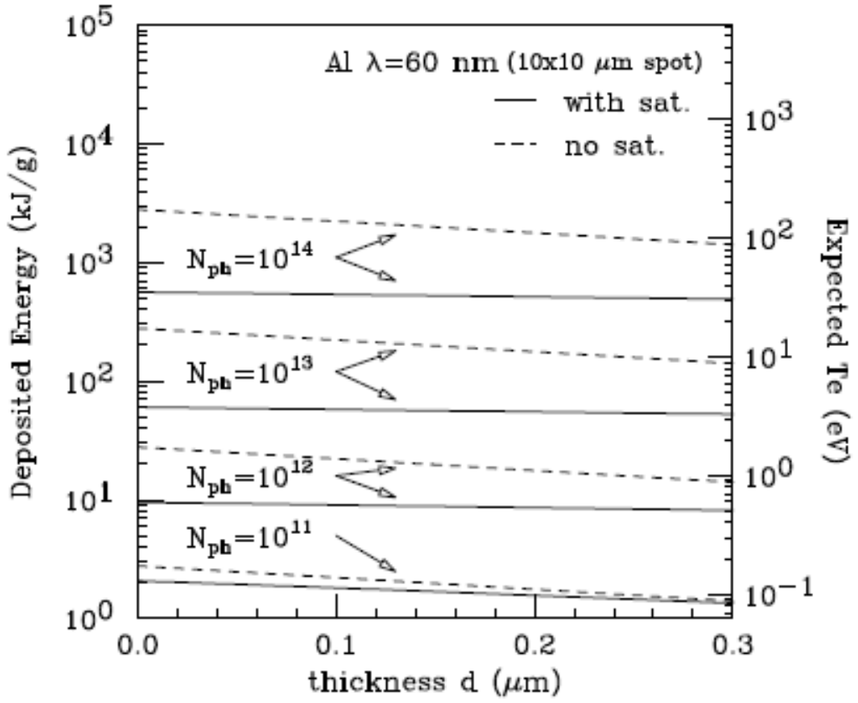

Figure 3. Deposited energy (kJ per gram of substance) as a function of the thickness d for a thin aluminum foil, for different intensities of the FEL pulses (10^{11} to 10^{14}) at a wavelength of 60 nm (spot 10x10 μm). The dashed curves are obtained without considering saturation effects due to the intensity of the pulse. The solid curves are obtained using a simple model for saturation. Saturation is expected to provide for high pulse intensities a much more uniform bulk heating (see flatness of the solid curves) and a decreased deposited energy. The expected electron temperature T_e is also shown.

Simple model for saturable absorption -compatible with exp. data taken at Flash (Hamburg)

$$dI(x) = -\frac{\alpha_s I(x) dx}{(1 + I(x)/I_{sat})}.$$

$$N_{sat} = K n_{el}$$

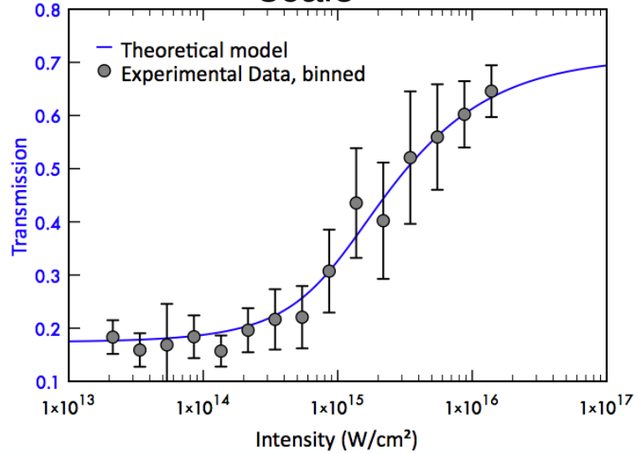

nature physics
ARTICLES
PUBLISHED ONLINE: 26 JULY 2009 | DOI: 10.1038/NPHYS1341

Turning solid aluminium transparent by intense soft X-ray photoionization

Bob Nagler *et al.**

Bulk heating with FEL1

- Quasi-isotherm bulk heating can be obtained by using FEL1 pulses on several films (Al, Si, Ge, and more)
- Electron temperatures are estimated to be in the range 1-10 eV (WDM regime)
- Large-sized (up to 2 cm) films are robust (0.1-0.3 microns thickness) and can be used for shot-to-shot experiments at the FEL repetition rate
- FEL2 useful for bulk heating of some important material (C for example)
- → Soft x-ray FELs are really useful for efficient bulk heating!

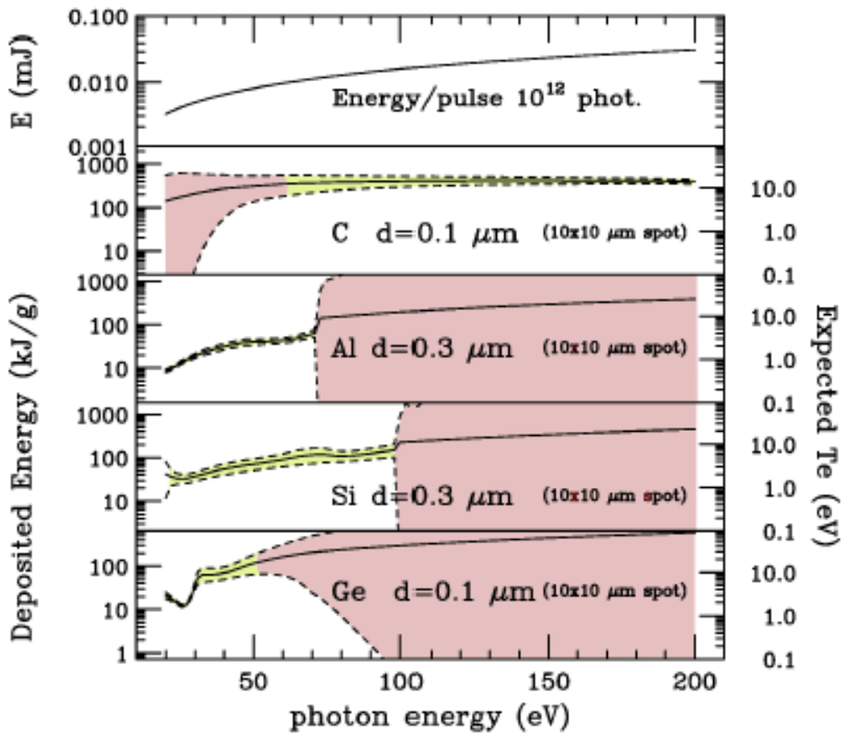

Figure 4. In the lower four panels we report the deposited energy (kJ per gram of substance) in different thin film materials as a function of the photon energy for a pulse containing 10^{12} photons (spot 10x10 μm). The deposited energy (solid curves) has been calculated accounting for possible saturation effects and show different trends according to the particular foil under consideration. The dashed curves represent the limits for the spread of deposited energy inside the films, so uniform bulk heating is obtained when the dashed curves define a narrow region (light green, color on-line). On the other hand, when most of the energy is deposited near the surface of the thin film, an extremely inhomogeneous heating is obtained (pink regions, color on-line). The expected electron temperature T_e is also shown on the right axis, showing that average temperatures in the 1-10 eV range are easily reached depending on the energy and thin foil material. The upper panel reports the pulse energy (mJ) as a function of the photon energy (eV) obviously changing of 1 order of magnitude from 20 to 200 eV. The FEL1 source (12-62 eV) turns out to be extremely efficient for obtaining uniform bulk heating of various materials (for example Al, Si, Ge shown in the picture).

Diagnostic developments

Nuclear Instruments and Methods in Physics Research A 621 (2010) 643–649

A method for estimating the temperature in high energy density free electron laser experiments

Emiliano Principi [a], Carino Ferrante [b], Adriano Filipponi [b], Filippo Bencivenga [c], Francesco D'Amico [c], Claudio Masciovecchio [c,*], Andrea Di Cicco [a,d]

[a] CNISM, Dipartimento di Fisica, Università degli Studi di Camerino via Madonna delle Carceri, I-62032 Camerino (MC), Italy
[b] Dipartimento di Fisica, Università degli Studi dell'Aquila, Via Vetoio, I-67100 L'Aquila, Italy
[c] Synchrotron ELETTRA, Strada Statale 14-I-34149 Basovizza, Trieste, Italy
[d] IMPMC, Université Paris 6, CNRS, 140 rue de Lourmel, 75015 Paris, France

ARTICLE INFO

Article history:
Received 19 February 2010
Received in revised form
24 March 2010
Accepted 24 March 2010

Keywords:
Temperature measurements
Pyrometer
Femto-second experiments
Warm dense matter
Heat equation

ABSTRACT

Present and forthcoming free electron laser (FEL) large scale facilities deliver high fluence ultrafast soft and hard X-ray pulses able to create and probe warm dense matter (WDM). Proper diagnostic for basic physical quantities, like temperature and density, is necessary, but the short lifetime of the WDM state (few ps) makes their measurements a challenging task. In this work we propose a method to estimate the WDM temperature using the experimental information from a slow temperature pyrometric probe exploiting the properties of the heat diffusion equation. Numerical simulations show that for typical thin foil samples, a temperature measurement with 1–10 μs temporal resolution at the distance of about 300–500 μm from the beam center contains sufficient information to retrieve the initial spatial temperature distribution with sufficient accuracy providing information on the temperature reached in the WDM regime. The inversion of the experimental information is obtained by means of a Bayesian approach exploiting a Metropolis Monte Carlo numerical procedure. The model and calculations presented in this work provide the theoretical background for the development of a device for temperature diagnostics of the TIMEX end-station at the Fermi@Elettra FEL facility.

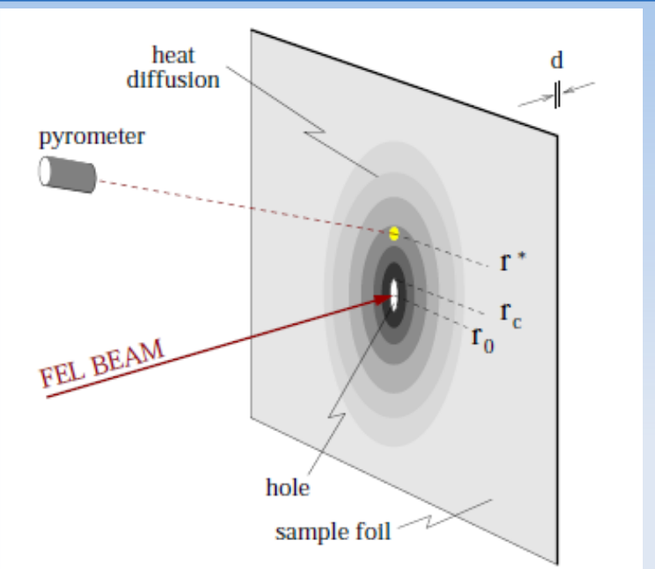

Figure 1: Experimental geometry.

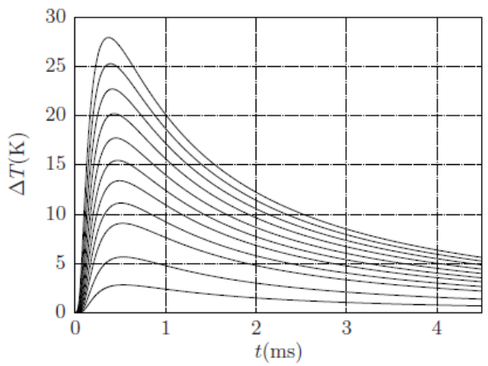

Figure 5: Temporal evolution of the temperature $\Delta T = T(t) - T_{bkg}$ at $r^* = 512$ μm for increasing peak temperature T_{max}, equal to T_{max} =1000, 1500, 2250, 3375, 5062, 7593, 11390, 17085, 25628, 38443, and 57665 K.

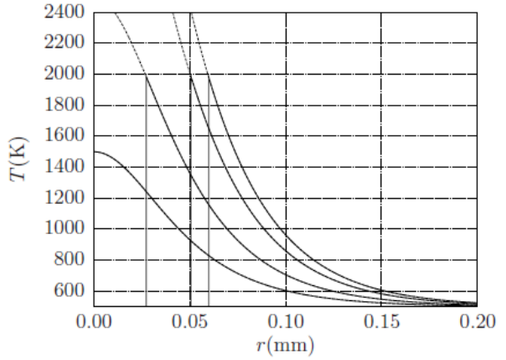

Figure 2: Examples of initial temperature profiles for increasing T_{max} equal to 1500, 2500, 4000 and 5000 K, $\xi \simeq 34$ μm, T_{bkg} = 500 K and T_{evap} = 2000 K. In the first curve $T_{max} < T_{evap}$ and the complete profile is visible, in the other cases the temperature profile begins at the hole boundary $r = r_c$ and is reported as a dashed curve for $r < r_c$.

Test of the infrared pyrometer

A low-cost infrared pyrometer (cassegrain design) has been realized. Cassegrain pyro: spot ~100-200 μm, 35 cm focus distance

Laser Pump: ~120 fs, 400 nm, ~60 μm spot

Sample pre-heated (580 K) with halo lamp.

Alignment with a long-distance microscope (Questar CM1)

Detection of temperature rise on the back of a Fe foil to avoid scattering of the pump pulse.

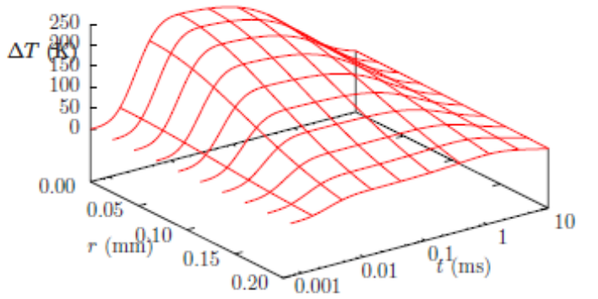

Figure 2: Temporal evolution of the radial temperature profile in the rear side of the sample for a Gaussian pulse with standard deviation $s = 0.1$ mm, and 1 mJ of absorbed energy, sample thickness $d = 10$ μm, and thermal diffusion $D = 5\ 10^{-6}$ m^2/s.

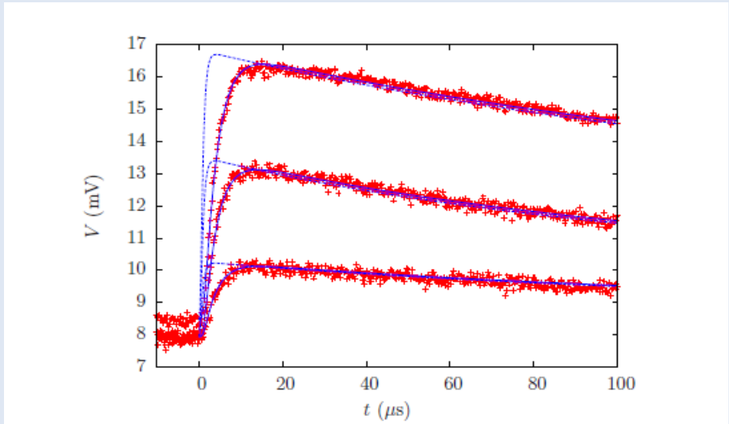

Figure 4: Temporal evolution of the simulated pyrometer sensor readout V, calculated for $d = 5$ μm, $R = 50$ μm, $D = 4.4\ 10^{-6}$ m^2/s. The three experimental data sets refer to increasing laser pulse energies of 1.2, 2.0 and 2.9 mJ. The corresponding base temperatures for the simulation were $T_0 = 581, 582, 589$ K respectively. The laser focal spot standard deviation was $s = 39$ μm ($s = 55$ μm for the 2.9 mJ pulse). The absorbed energies E were 15, 28, and 58 μJ respectively. Dashes lines are the voltage predictions without accounting for the detector/amplifier time response. The bottom figure is the same comparison on a logarithmic t scale.

TIMEX end-station: present status

- **Design of the end-station and place of orders completed in June 2010. Vacuum chambers delivered in late October 2010. Assembling and test of the main components of the TIMEX end-station in the main Fermi hall started in December 2010.**
- **Problems: the TIMEX optics (C. Svetina, D. Cocco) did not match specifications (SESO manifacturing) and are still under construction. No focusing optics is still available!**
- **Interlock systems, remote controls, hardware interfaces and collection software are currently under development in collaboration with the machine group. A special diagnostics for ultrafast high-temperature measurements is under test and construction (E. Principi).**
- **Tests for the first runs of the Fermi@Elettra in March/July 2011 have been carried out in a simplified configuration (no focusing).**
- **Personnel: a scientist and a PhD for the end-station has been recruited. Current personnel (Camerino, L'Aquila, Sincrotrone Trieste): F. Bencivenga, F. D'Amico, A. Di Cicco, A. Filipponi, A. Gessini, E. Giangrisostomi, R. Gunnella, C. Masciovecchio, E. Principi.**

Web site: http://gnxas.unicam.it/TIMEX

Assembling the TIMEX UHV chamber in the main Fermi hall (17 nov 2010)

TIMEX first tests

- Temporary installation with mirror providing ~300 μm spot
- 65 nm (~19 eV) ~200 fs radiation
- Beamtime used for alignment and for measuring the pulse energy (peak ~0.2 μJ on the detector → ~1 μJ at source) compatible with expected performance of FEL1 at this early stage of commissioning
- Laser seed signal (4.8 eV) important (~1μJ per shot (removed with Al 0.3 μm filter)

-Detector: Si photo-diode SXUV100 (IRD)
-Saturation induced by the 0.2 ps pulses.
- The time integral of the traces, divided by 50 Q, is the collected charge (0.1-1 nC with Al filter),corresponding to 0.18 μJ peak energies

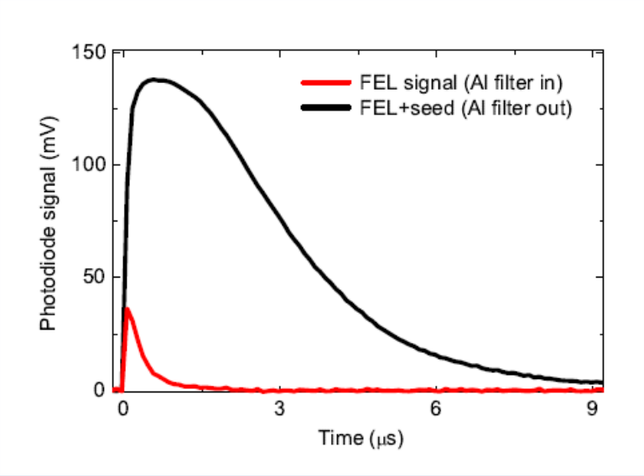

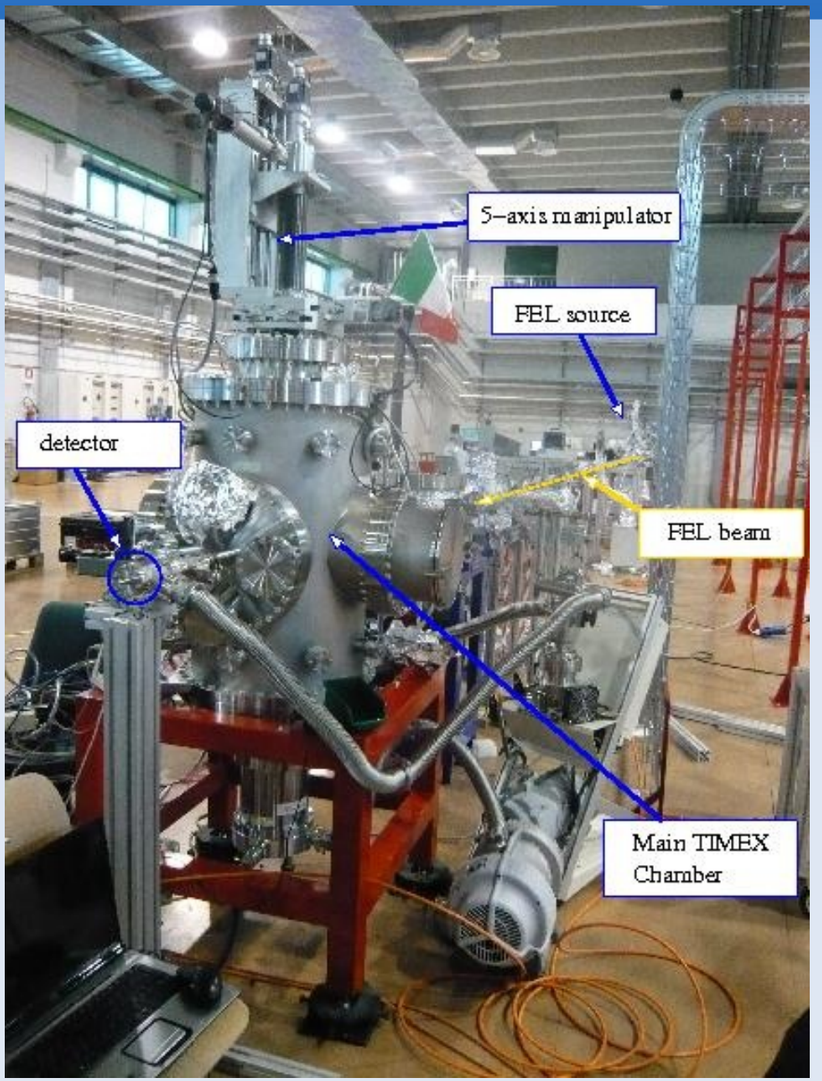

Timex first experiments

- *In 2012 we plan to develop and exploit two main experimental configurations:*
- *1) transmission (saturation at different fluencies, wavelengths, use of higher harmonics) and UV/soft x-ray reflectance*
- *2) pump & probe with optical probe (optical reflectance/transmission)*

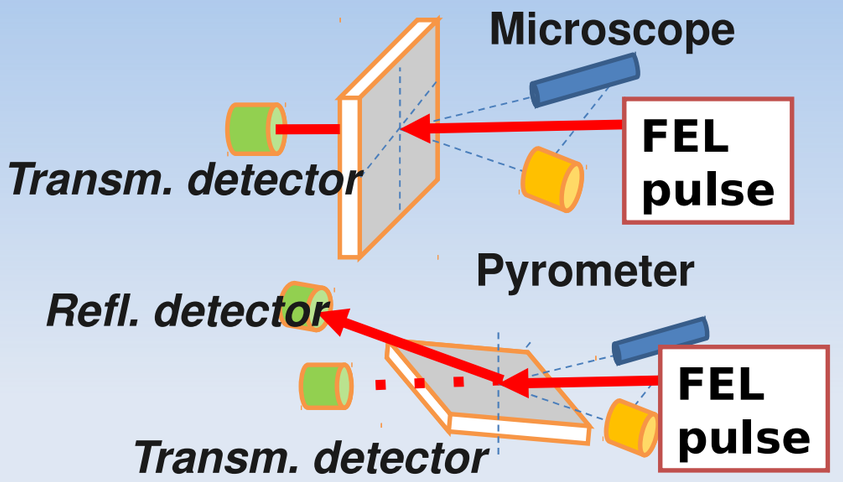

Planned experiments include:

- *Saturation effects and phase transitions induced by FEL pulses in selected materials (see figure)*
- *Absorption on free-standing foils as a function of the pulse fluence and time duration (both first and higher harmonics)*
- *Reflection on surfaces of selected materials as a function of the fluency and pulse duration*

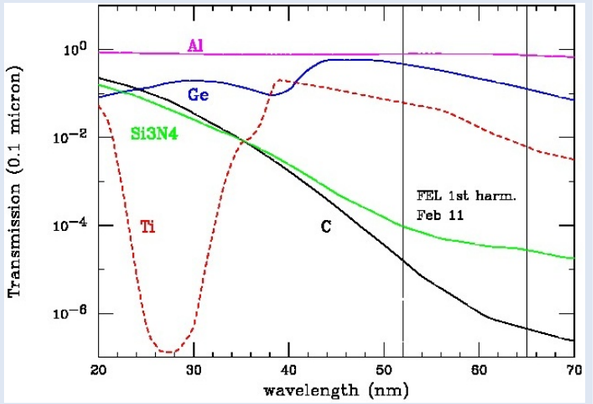

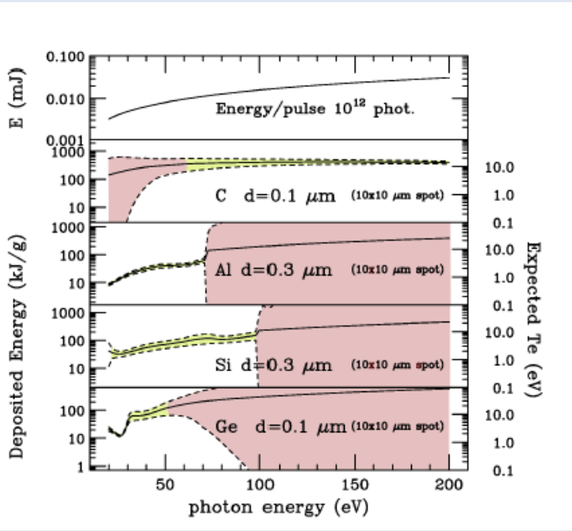

Pump&Probe: Pilot ultrafast experiment with a laser source

- Pump-and-probe reflectivity measurements on a fresh Si(100) surface (moderately B-doped, p-type, concentration below 10^{16} cm $^{-3}$)
- Laser source: pump at 400 nm, pulse width FWHM 80 fs, 500 Hz
- Typical pump spot size 100 μm (pump) and 50 μm (probe).
- Super-continuum 350-800 nm probe, probing depth around 10 nm.

P&P set-up: Time resolved optical spectroscopy

- transient transmittance (absorbance) or reflectivity of the sample
- 50 fs/3 nm time/spectral resolution, spectral range 350 – 1000 nm
- shot-to-shot detection, <10^{-3} OD sensitivity
- observing in real-time the non-equilibrium dielectric function

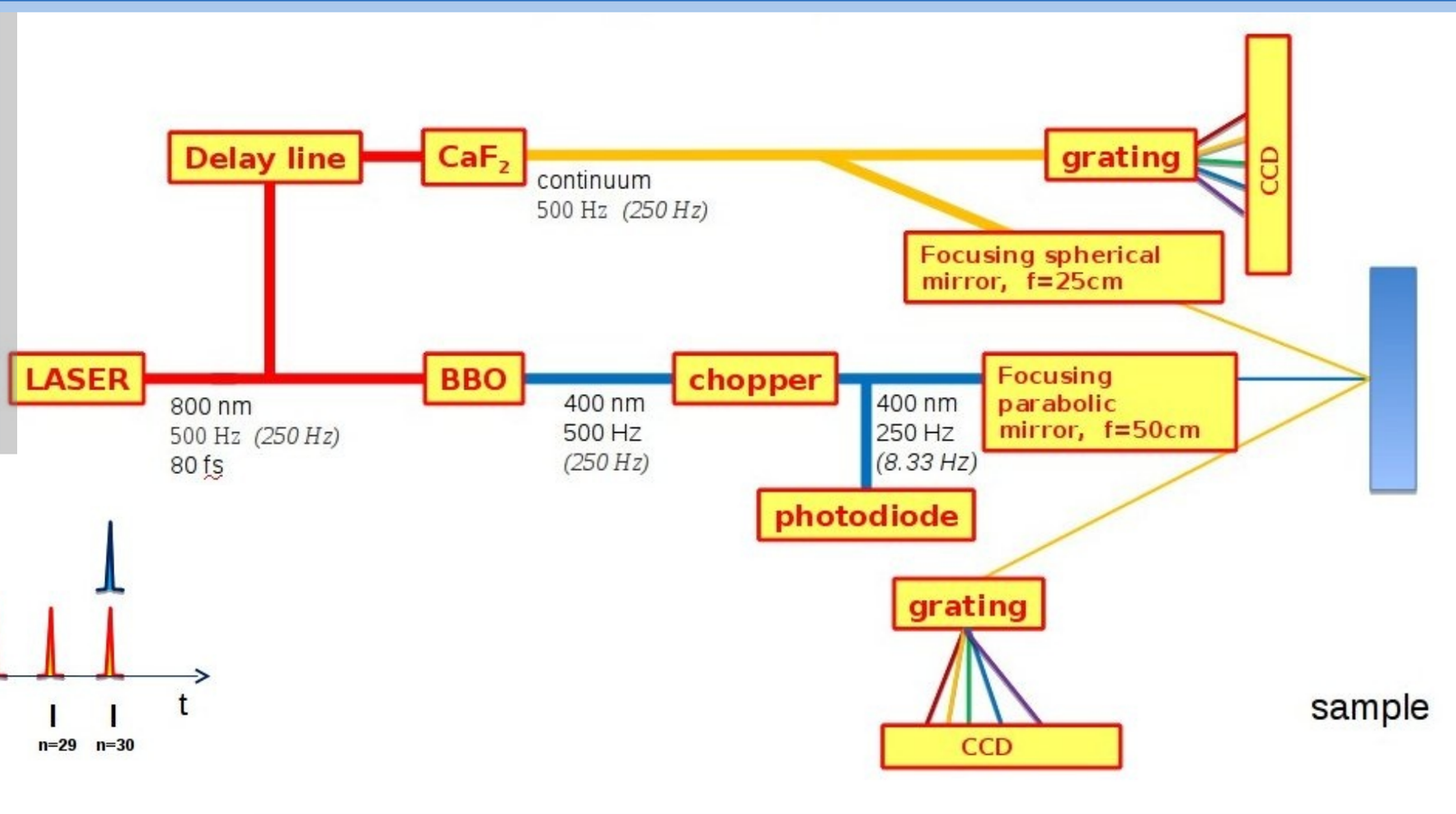

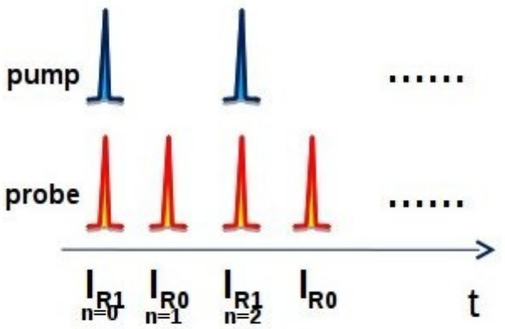

Normal repetition rate

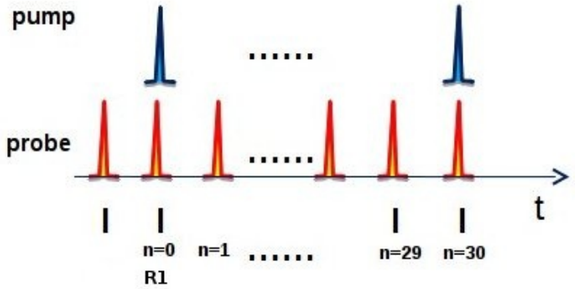

Single-shot configuration

Amplified Ti:Sapphire laser source: 800 nm, 80 fs, 2W, 1 kHz.

Previous ultrafast experiments

·Si has an indirect gap (1.12 eV) so excitation with lasers with wavelengths λ > 364 Ang. Involve multi-photon and phonon-assisted transitions.

· At low laser fluencies a moderate negative change of the reflective was obtained.

·A positive reflectivity change within 200 fs is observed at high fluencies using P&P ultrafast techniques.

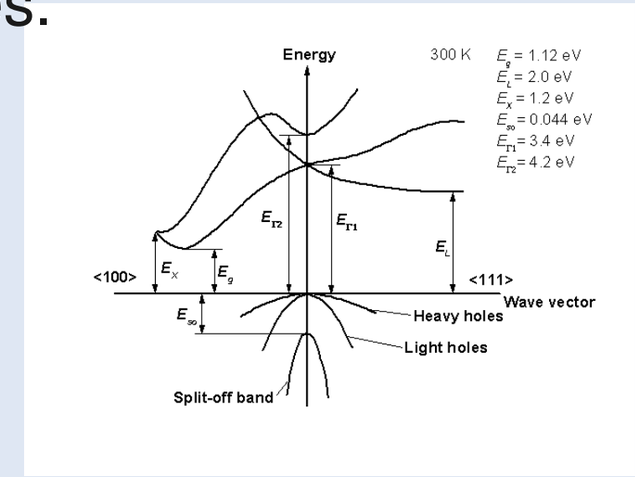

VOLUME 50, NUMBER 6 PHYSICAL REVIEW LETTERS 7 FEBRUARY 1983

Time-Resolved Reflectivity Measurements of Femtosecond-Optical-Pulse–Induced Phase Transitions in Silicon

C. V. Shank, R. Yen, and C. Hirlimann
Bell Telephone Laboratories, Holmdel, New Jersey 07733
(Received 29 November 1982)

The reflectivity of silicon has been measured following excitation with intense 90-fsec optical pulses. These measurements for the first time clearly resolve in time the process of energy transfer to the crystal lattice and the dynamics of the phase transition to the melted state.

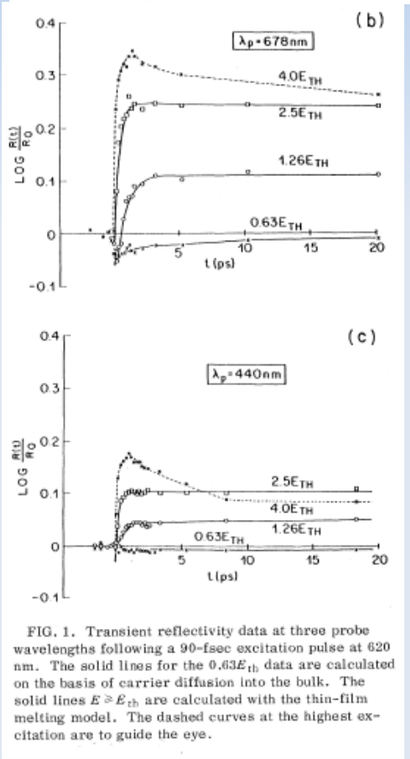

FIG. 1. Transient reflectivity data at three probe wavelengths following a 90-fsec excitation pulse at 620 nm. The solid lines for the $0.63E_{th}$ data are calculated on the basis of carrier diffusion into the bulk. The solid lines $E \geq E_{th}$ are calculated with the thin-film melting model. The dashed curves at the highest excitation are to guide the eye.

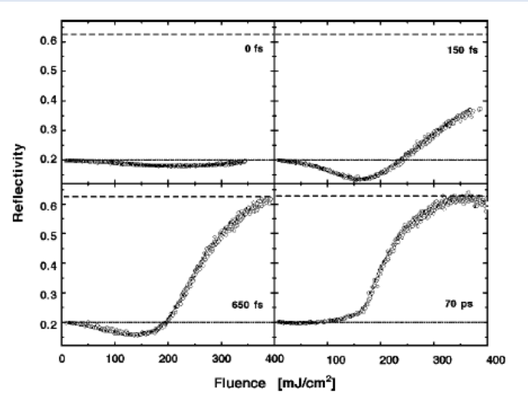

FIG. 2. Reflectivity of silicon as a function of excitation fluence for four different delay times, 625-nm wavelength, 49° angle of incidence, and *p* polarization. The dotted and dashed lines mark the reflectivity of solid and liquid silicon, respectively.

PHYSICAL REVIEW B VOLUME 61, NUMBER 4 15 JANUARY 2000-II

Generation of dense electron-hole plasmas in silicon

K. Sokolowski-Tinten and D. von der Linde
Institut für Laser- und Plasmaphysik, Universität-GHS-Essen, D-45117 Essen, Federal Republic of Germany

Non-thermal melting

·The positive reflectivity change is associated with a rapid melting process.

·The sudden laser-induced excitation of a large fraction of valence electrons into the conduction band changes the potential energy landscape.

· Tight-binding calculations show that the minimum associated with the diamond structure becomes a saddle point and within 100 fs atoms are displaced of about 1 Ang. (15% valence electron plasma) with average increase of temperature around 0.3 eV leading to melting (critical density estimated around 10^{22} cm $^{-3}$)

·The dramatical ultrafast weakening of the bond is confirmed by ab-initio MD calculations predicting a metallic liquid within 100-200 fs.

PHYSICAL REVIEW B VOLUME 49, NUMBER 11 15 MARCH 1994-I

Time dependence of the laser-induced femtosecond lattice instability of Si and GaAs: Role of longitudinal optical distortions

P. Stampfli* and K. H. Bennemann
Theoretical Physics, Freie Universität Berlin, Arnimallee 14, D-14195 Berlin, Germany

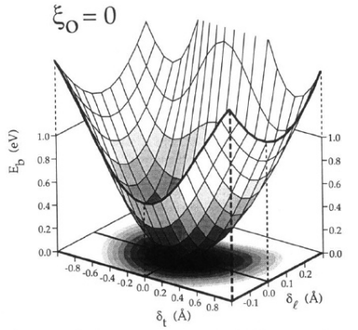

FIG. 2. Cohesive energy per atom E_b of Si [Eqs. (1)–(5)] in the absence of an electron-hole plasma ($\xi_0=0$) shown as a function of the transverse acoustic distortion δ_t and the longitudinal optical distortion δ_l of the diamond lattice. Here the ideal diamond structure ($\delta_t=\delta_l=0$) is a stable minimum of the cohesive energy.

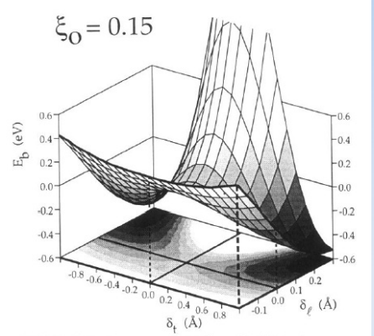

FIG. 3. Cohesive energy for Si [Eqs. (1)–(5)] in the presence of an electron-hole plasma of density $\xi_0=0.15$ corresponding to the excitation of 15% of the valence electrons into the conduction band. We use the same representation as in Fig. 2. Note that the ideal diamond structure ($\delta_t=\delta_l=0$) has become an unstable saddle point.

VOLUME 77, NUMBER 15 PHYSICAL REVIEW LETTERS 7 OCTOBER 1996

***Ab initio* Molecular Dynamics Simulation of Laser Melting of Silicon**

Pier Luigi Silvestrelli,[1] Ali Alavi,[2] Michele Parrinello,[1] and Daan Frenkel[3]

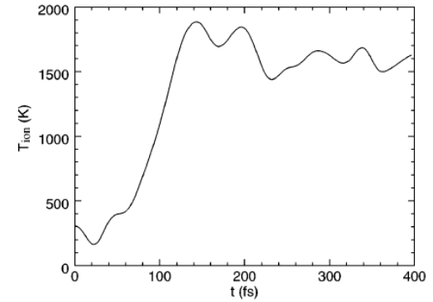

FIG. 1. Time dependence of the instantaneous ionic temperature, defined as $T_{\rm ion}(t) = [M/(3N-3)k_B]\sum_{I=1}^{N} v_I^2(t)$, where k_B is the Boltzmann constant, M is the Si ion mass, and $v_I(t)$ the ionic velocity at time t.

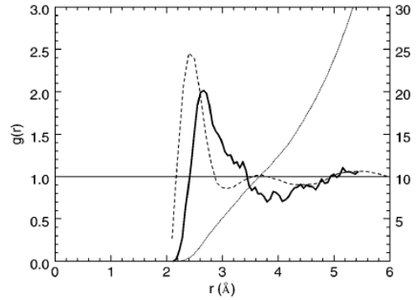

FIG. 3. Pair correlation function $g(r)$. Solid line: MD simulation. Dashed line: experimental result [19] for l-Si. Dotted line: coordination number $N(r)$.

Ultrafast excitation of the Si(100) surface: pictorial view

·A combined MC and MD calculation on a (100) slab of 142560 atoms was used to calculate the thermodynamic pathway after excitation (500 fs pulse). Rapid non-thermal disordering and nearly isochoric heating (B) of the metallic liquid is followed by cooling in the liquid-vapor regime.

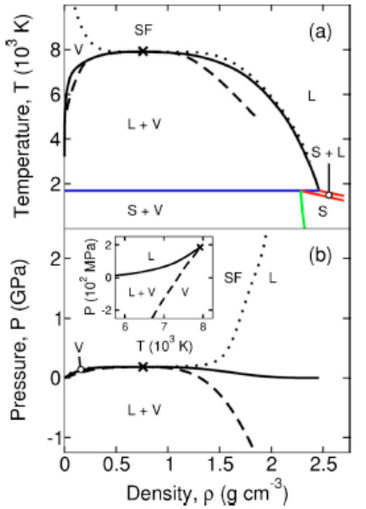

FIG. 3. (Color online) Phase diagram of silicon: (a) ρ-T plane; (b) ρ-P plane; inset: T-P plane. Black solid line: binodal (liquid-vapor coexistence); blue: triple line (solid-liquid-vapor coexistence); green: solid-vapor coexistence line; red: solid-liquid coexistence lines; dotted line: critical isobar and isotherm; dashed line: spinodal; cross: critical point. *S*: solid; *L*: liquid; *V*: vapor; *SF*: supercritical fluid (for $T>T_c$ and $P>P_c$). See text for details.

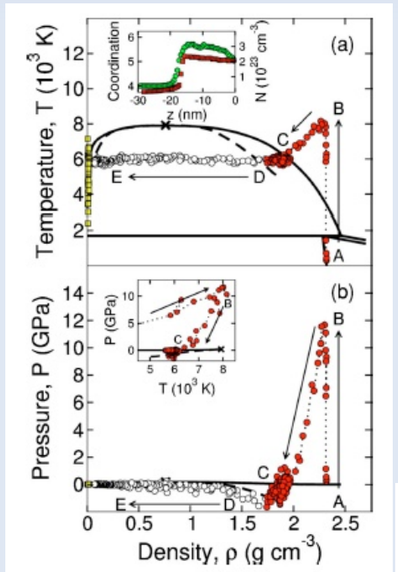

FIG. 5. (Color online) Time evolution of the system in the (a) ρ-T and (b) ρ-P planes for a 500 fs pulse at a fluence $F=F_{th}^{fs}=0.225$ J cm^{-2}; the trajectory is for a region of the target initially at a depth of 4 nm below the surface. White circles and dotted line: macroscopic branch; red circles: dense branch; yellow squares: gas branch. Arrows indicate the flow of time. Capital letters refer to locations in the phase diagram (see text). Insets: (a) coordination (green circles) and electron density N (red squares) as a function of distance from the surface z at $t=1$ ps (note the change in properties across the solid-liquid interface at $z\approx-18$ nm); (b) view of the trajectory in the T-P plane.

PHYSICAL REVIEW B 73, 134108 (2006)

Thermodynamic pathways to melting, ablation, and solidification in absorbing solids under pulsed laser irradiation

Patrick Lorazo,[1,2] Laurent J. Lewis,[2,*] and Michel Meunier[1,†]

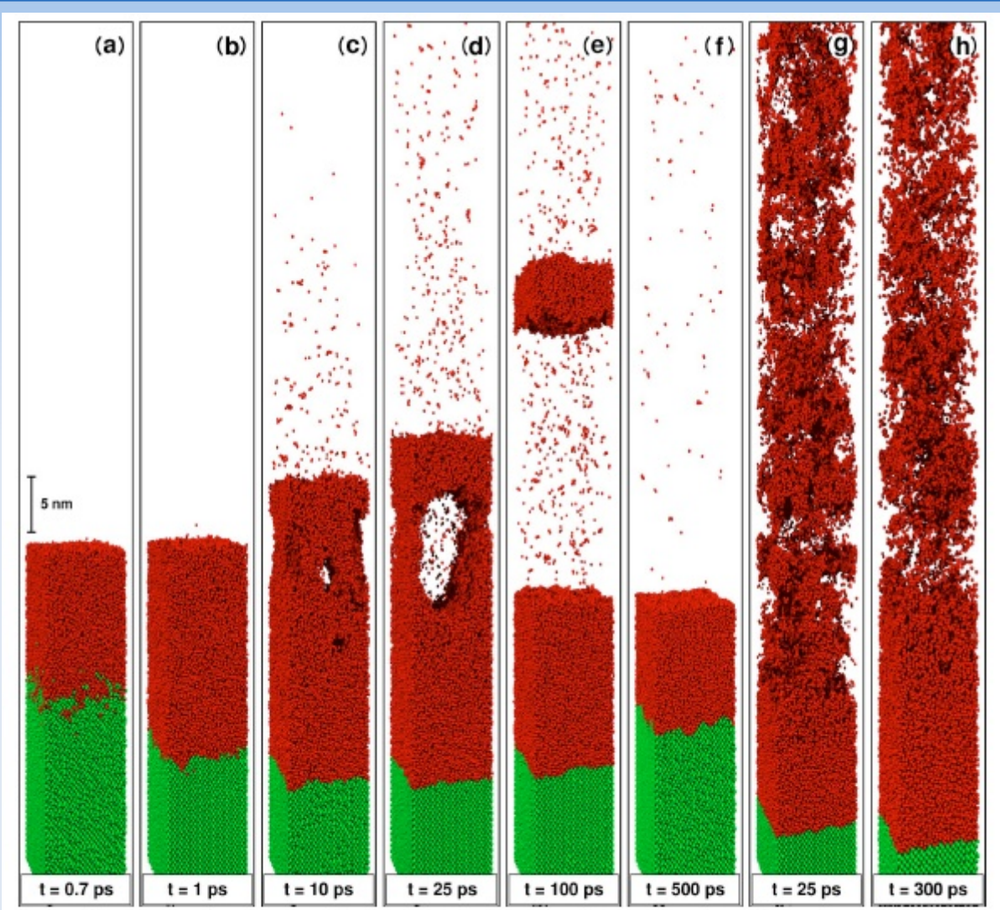

FIG. 4. (Color online) Snapshots revealing the structural changes induced in a Si(100) substrate by 500 fs and 100 ps pulses at 266 nm: (a)–(f) 500 fs pulse at a fluence $F=F_{th}^{fs}=0.225$ J cm^{-2}; (g) 500 fs pulse at a fluence $F=2.2F_{th}^{fs}=0.50$ J cm^{-2}; (h) 100 ps pulse at a fluence $F=1.1F_{th}^{ps}=0.45$ J cm^{-2}; F_{th}^{fs} and F_{th}^{ps} are the ablation thresholds under femtosecond and picosecond irradiation, respectively. Green: (semiconducting) crystalline silicon; red: (metallic) liquid silicon. Each pulse begins at $t=0$.

Damage threshold

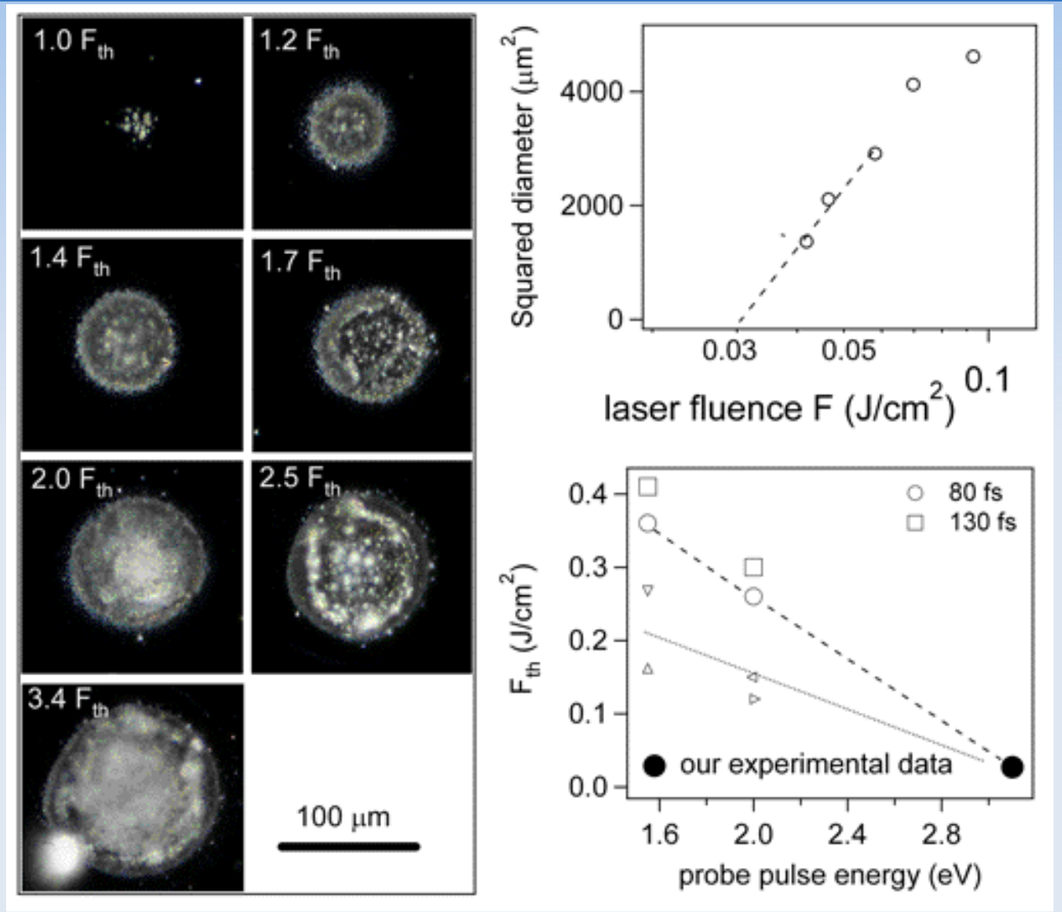

Optical microscope images of the Si(100) surface for different pulse intensity. The damage threshold (F_{Th}) is in line with previous estimates.

From *S. K. Sundaram and E. Mazur, Nat. Mat. 1, 217 (2002).*

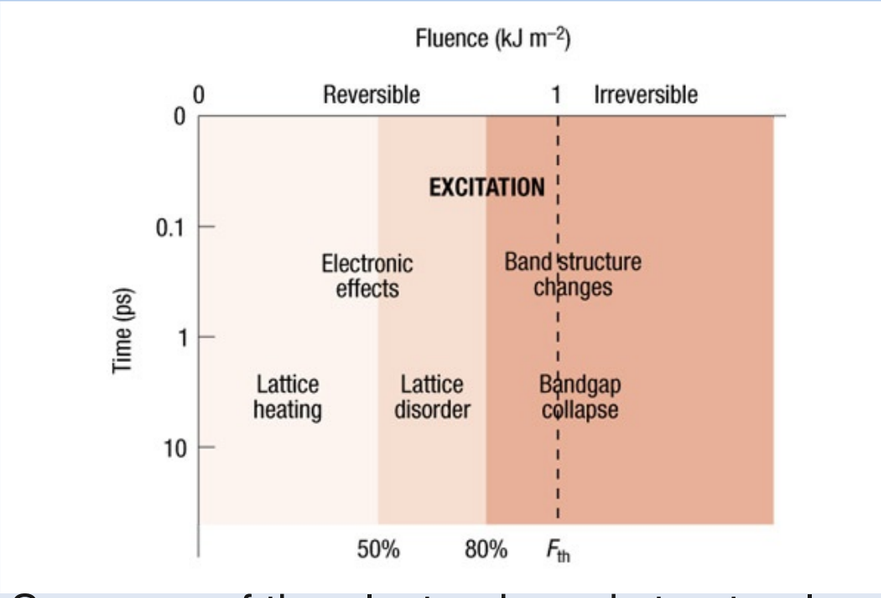

Summary of the electronic and structural effects after excitation with short laser pulses (direct-gap GaAs). Excitations range from 0.1 to 2.0 kJ m-2 . Three shaded regions indicate three distinct regimes.

Pump energy below the damage threshold

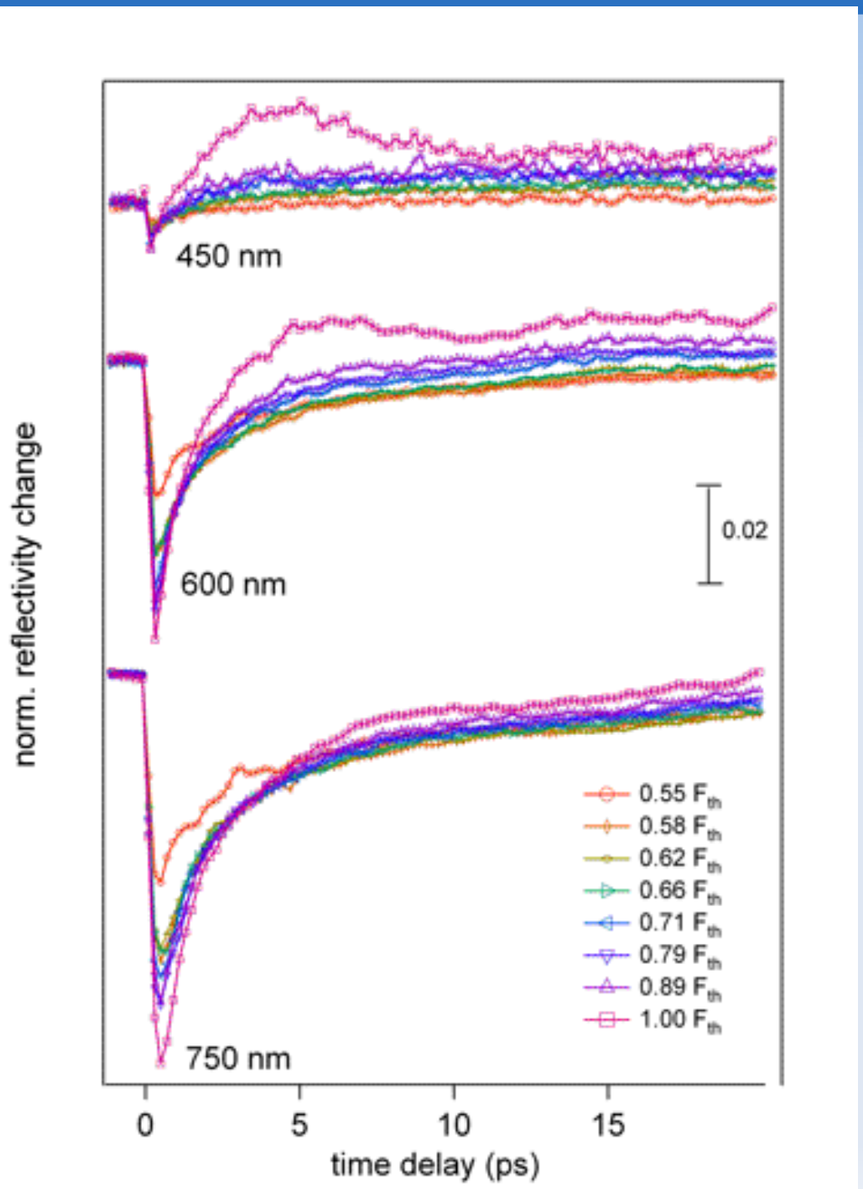

- **Ultrafast changes in Si(100) reflectivity strongly depend on the (probe) wavelength.**
- **Strong negative variations increasing with fluence from 1% to 10% (long wavelengths) within 1 ps, gradual recovery at times ~500 ps.**

- **The reflectivity change tends to be positive (after 1ps at 400 nm, above 20 ps for longer wavelength).**

Summary of Si(100) optical ultrafast data 0.55-1.00 Th -below damage threshold-

Negative reflectivity change in red, positive in green. Time scale 0-20 ps.

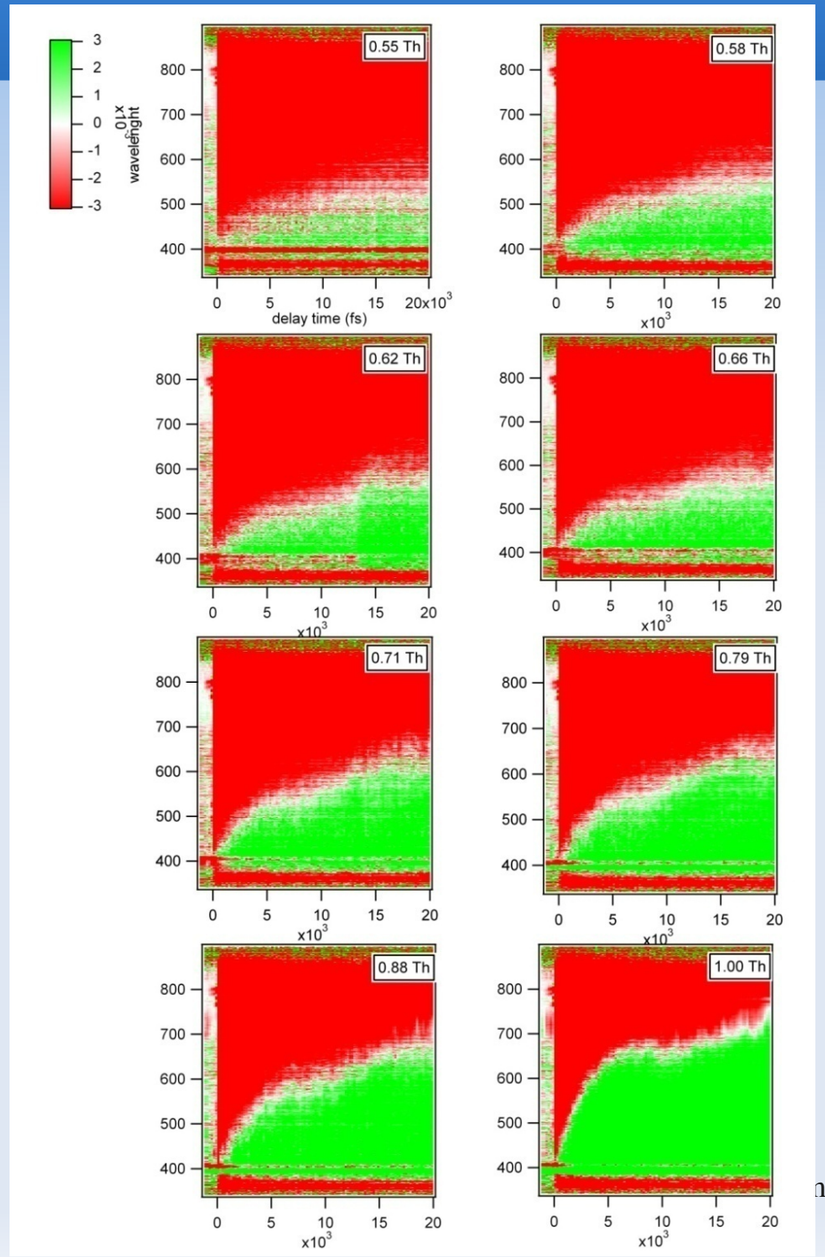

Negative reflectivity change in red, positive in green. Time scale 0-500 ps.

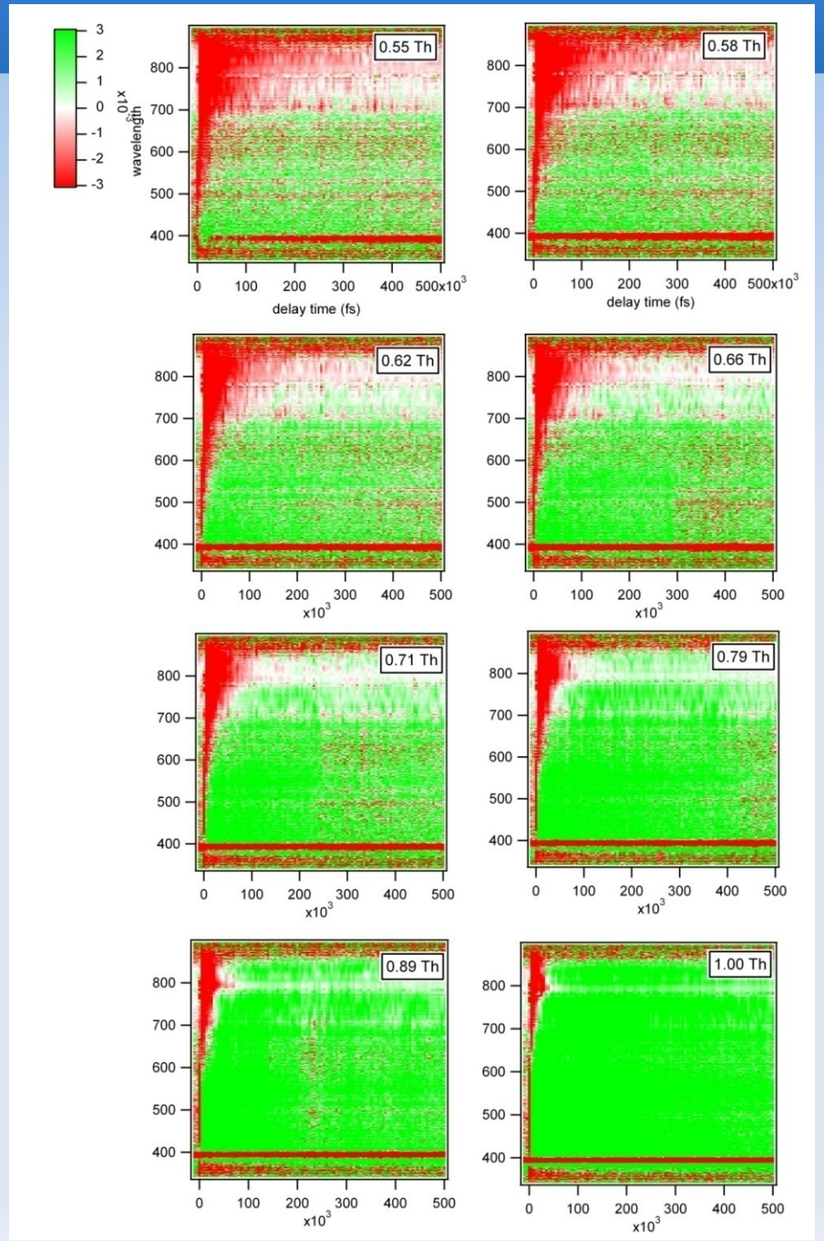

Time profile above threshold

·Above a critical threshold for the pulse intensity the reflectivity change is positive at all wavelengths within 300 fs. The positive change reaches its maximum (about 50%) within ~ 3 ps and then a slow decrease is observed up to ~300 ps.

·Only single-shot measurements are possible because the Si(100) surface is irreversibly damaged.

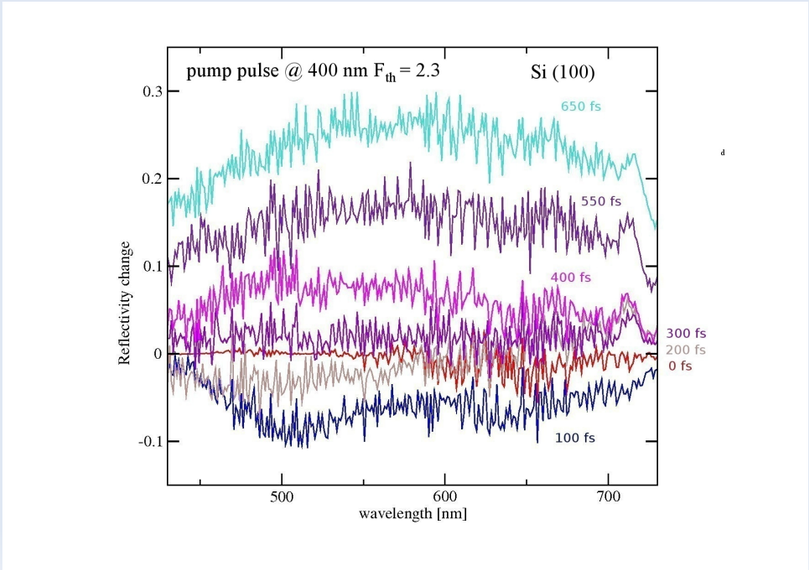

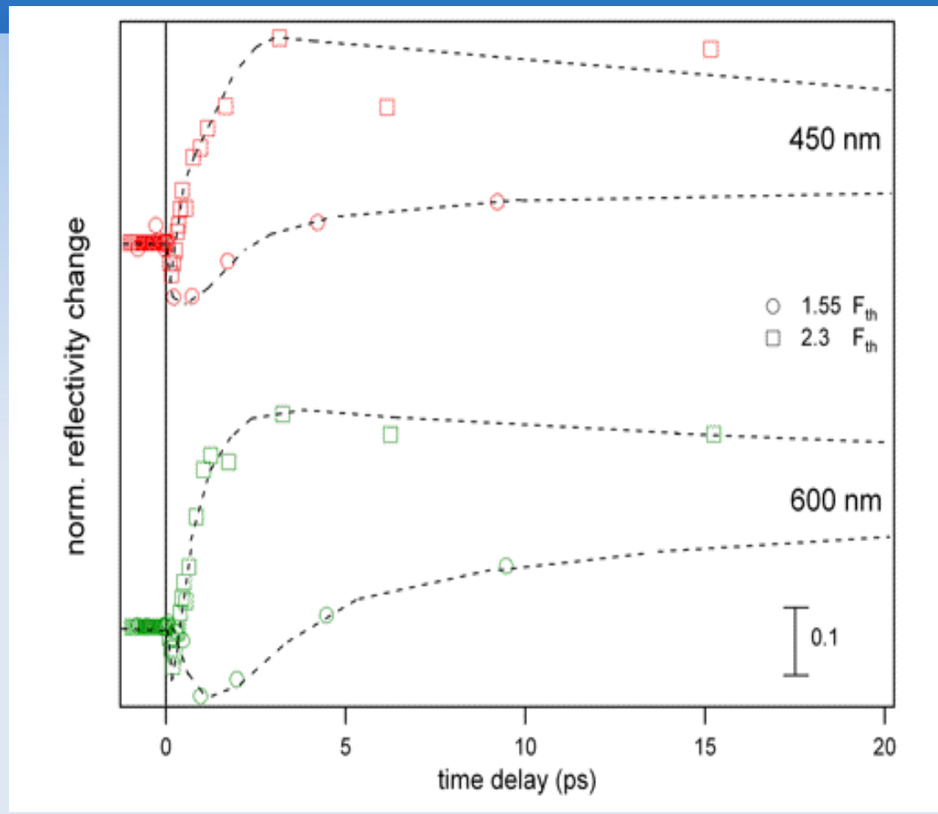

Trend for ultrafast reflectivity

Changes in reflectivity can be calculated modelling the dielectric function (refraction index n).
The change depends mainly on the (time-dependent) number density N(t) of excited electrons and on the electron temperature Te.
The number density N(t) at short times is well described by an exponential decay of the initial excitation density N_{in} (relaxation time t~10 ps). The excess energy of about 1.8 eV (hv-Eg) correspond to initial temperatures up to 20000 K for the electrons. The hot carriers thermalize with the lattice with a time constantt $\tau_{el\text{-}ph}$ ~260 fs (PRB vol. 66, 165217).

For our temporal resolution (100 fs) we expect to see 3 contributions:

1) free-carrier (FC) contribution (Drude-like)
– *negative*
2) state-filling (SF) associated with the absence of electrons in the valence band, lowering the absorption coefficient
- *negative*
3) lattice heating effects as a consequence of electron thermalization (variation of the refraction index with temperature)
-*positive*

PHYSICAL REVIEW B **66**, 165217 (2002)

Femtosecond pump-probe reflectivity study of silicon carrier dynamics

A. J. Sabbah and D. M. Riffe
Physics Department, Utah State University, Logan, Utah 84322-4415

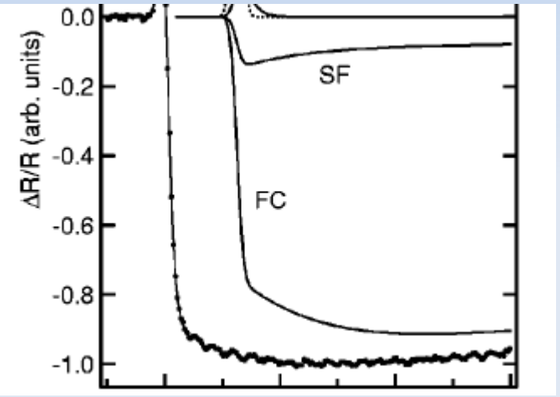

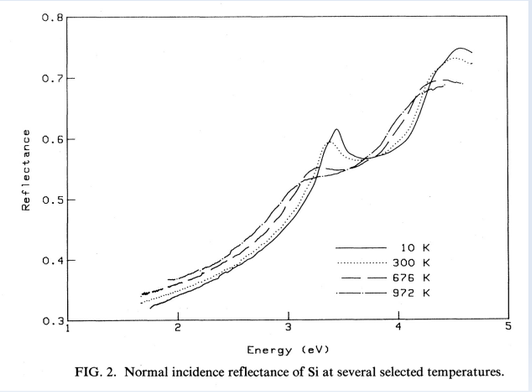

FIG. 2. Normal incidence reflectance of Si at several selected temperatures.

0.1 to 20 ps trend below threshold

Profile reproduced using time constants from literature and a lattice heating contribution corresponding to about 450 K (fluence 0.55 Fth).

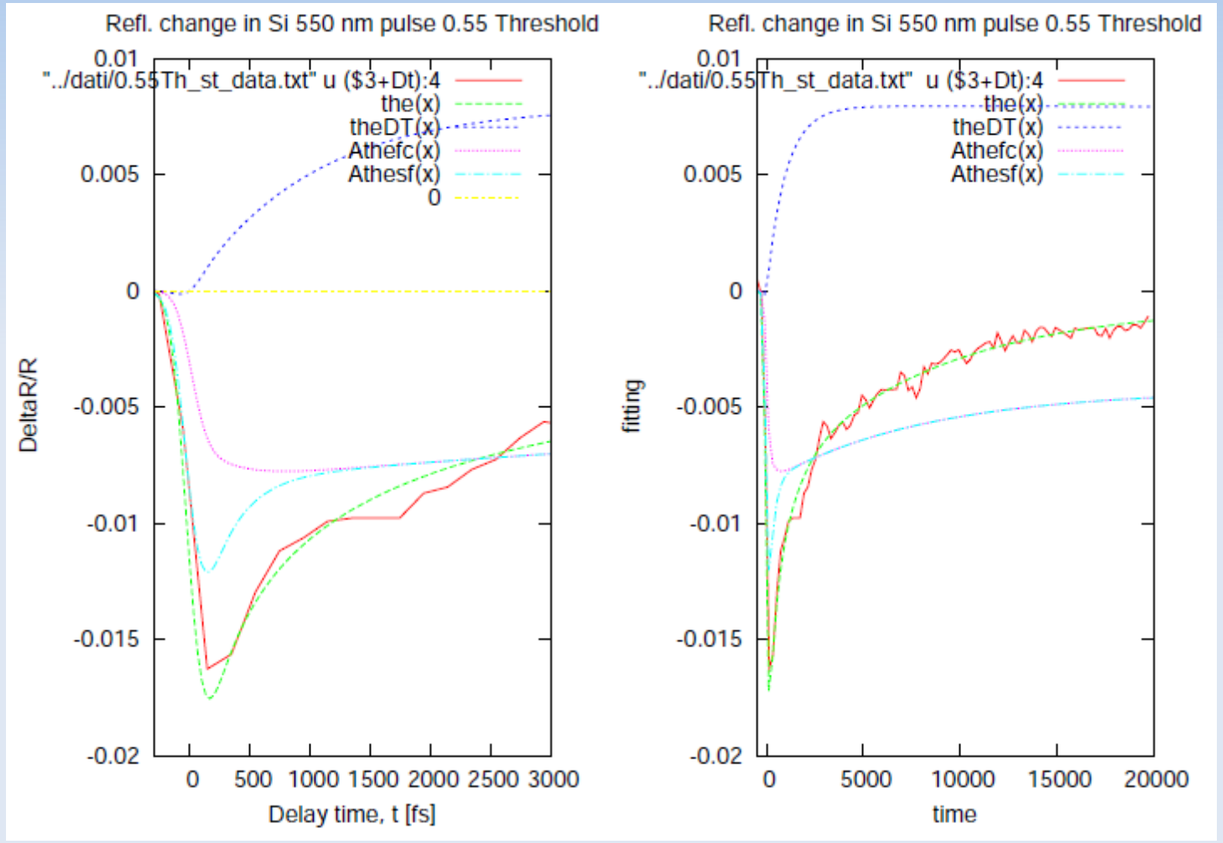

Ultrafast melting

Profile for high fluency reproduced using same time constants from literature and ultrafast melting taking place with a time constant of 260 fs (fluence 2.2 Fth).

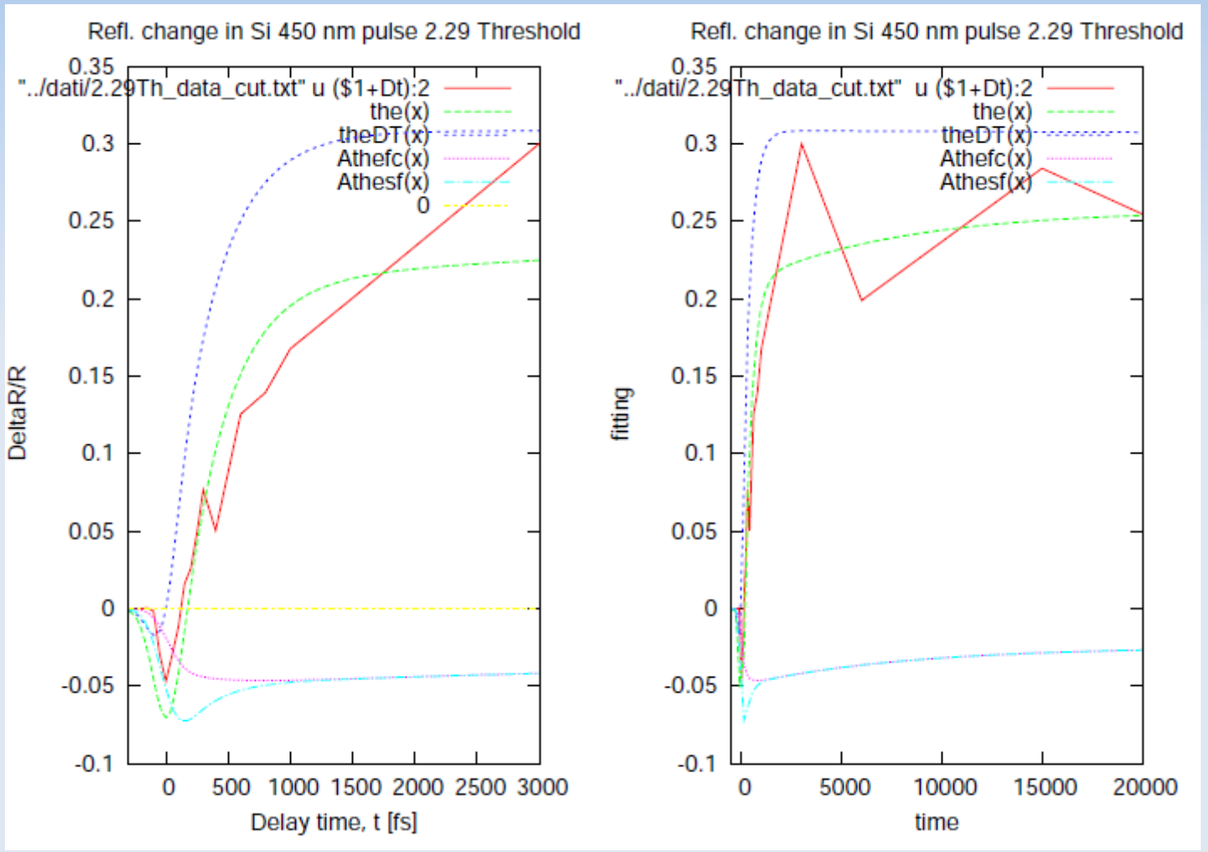

Conclusions

1. The Fermi@Elettra seeded Free Electron Laser source is available for users experiments (2012).
2. FEL sources open new opportunities for investigating extreme and non-equilibrium states in disordered matter.
2.The TIMEX end-station at the Fermi at Elettra facility is under commissioning with a specialized optics and will be dedicated to ultrafast studies of bulk matter under extreme conditions.
3. Ultrafast pump-and-probe pilot reflectivity experiments on Si show that useful information about the dynamics of phase transitions can be obtained. Non-thermal melting of Si takes place within 300 fs and is followed by lattice heating or melting within 3 ps, as a function of the pump fluence.

THANKS!